CHALMERS

Photo/copyright/Gunnar Britse/www.eco-photos.net/www.windpowerphotos.com

Estimation of wind energy production in relation to orographic complexity
A reliability study of two conventional computer software

Master of Science Thesis

KARL J. NILSSON

Gotland University
Passion & Science

Estimation of wind energy production in relation to orographic complexity

A reliability study of two conventional computer software

KARL J.NILSSON

Examiner: Doc. Ola Carlson
Supervisor: Dr. Stefan Ivanell

Gotland University
Passion & Science

Estimation of wind energy production in relation to orographic complexity:
A reliability study of two conventional computer software

Typeset in $\mathcal{AMS}$-LaTeX

Front cover illustration shows a photo of Näsudden located at Gotland, Sweden. Used with permission, [5].

Abstract

The aim with this thesis is to compare two wind simulation software to simulate energy production which are based on two different flow models; a linear and a non-linear. The test parameter is orographic complexity and the test software is WAsP, which is based on the linear model and WindSim, which is based on the non-linear model. The test sites are Näsudden and Hunnflen which have low orographic complexity and high orographic complexity respectively. At each site turbines with a long record of production are selected.

In a first step the basics of wind approximations, measurements and conversion is presented. The aim with this is to present the input data for the flow models but also to show how complex winds, and thus wind simulations, are. Thereafter, the flow models are presented briefly.

The simulation is performed by a preparation process in a third software called WindPRO and is followed by the actual simulations in the two simulation software. The results are then compared to measured production data of the chosen wind turbines.

The results indicate that WAsP and WindSim estimate the energy production at a similar level which is close to the measured production when the orographic complexity is low. The WindSim simulation is very time consuming when comparing it to the WAsP simulation. When it comes to high orographic complexity the results indicate that WindSim estimates the energy production in a very close range to the measured production. The WAsP simulation, however, overestimates the energy production with about 40%. In the case with high orographic complexity the results show that a flow model that can calculate turbulence is needed. The model used in WindSim can model turbulence and therefore estimates an accurate energy production.

Sammanfattning

Syftet med arbetet är att jämföra två vindsimuleringsprogramvaror som är baserade på två olika flödesmodeller; en linjär och en olinjär. Testparametern i simuleringarna är orografisk komplexitet och programvarorna som används är WAsP, som är baserad på den linjära flödesmodellen, samt WindSim, som baseras på den olinjära flödesmodellen. Två områden har valts ut för simuleringarna; Näsudden, vilket har en låg orografisk komplexitet och Hunnflen, vilket har en hög orografisk komplexitet. I båda dessa områden finns redan ett antal vindkraftverk installerade. Utifrån tillgänglig produktionsdata har ett verk i Näsudden valts ut; Siral, samt tre verk i Hunnflen valts ut; Ferdinand, Vilhelm och Freja.

I ett första steg i rapporten presenteras grundläggande information om energin i vinden genom vindapproximationer, mätningar och omvandling. Syftet med detta kapitel är dels att presentera vissa indata i flödesmodellerna samt ge en bild av hur komplex vinden och således vindsimulering är. Därefter presenteras de två flödesmodellerna och följs av en kortfattad jämförelse dessa emellan.

Simuleringsprocessen är indelad i två huvuddelar. Den första är preparering av en terrängfil som utförs i en tredjepartsprogramvara WindPRO. Den andra är själva simuleringarna som utgår från terrängfilen samt vinddata och utförs i respektive programvara. Terrängfilen samt vinddatan är således identiska i respektive programvara.

Resultatet jämförs sedan med uppmätt produktionsdata för respektive vindkraftverk. Resultaten pekar på att båda programvarorna uppskattar en energiproduktion som ligger mycket nära den uppmätta vid förhållanden då låg orografisk komplexitet föreligger. Simuleringen i WindSim tar mycket mer tid i anspråk än den i WAsP vilket ger en indikation på att WAsP är att föredra för simuleringar vid låg orografisk terräng. När det gäller hög orografisk komplexitet så uppskattar WindSim en energiproduktion som ligger mycket nära den uppmätta. WAsP överskattar dock energiproduktionen med ungefär 40%. I det här fallet pekar resultaten på att det krävs en modell som kan ta hänsyn till den turbulens som uppstår på grund av den höga orografiska komplexiteten. Modellen i WindSim kan modellera turbulens och uppskattar därför en precis energiproduktion.

Preface

This master of science thesis is the final project for a Master of Science degree of totally 270 ECTS in Mechanical Engineering at Chalmers University of Technology in Gothenburg, Sweden. The project was executed in Visby/Gothenburg 2009/2010 as a cooperation between Chalmers University of Technology and Gotland University within the field of wind energy engineering and corresponds to 30 ECTS. Examiner for the report is Doc. Ola Carlson, Chalmers University of Technology, and supervisor is Dr. Stefan Ivanell, Gotland University.

First, I would like to thank the staff, including my supervisor Dr. Stefan Ivanell, at the energy section at Gotland University for all the help with issues concerning the content of the thesis and for always making me feel welcome in Visby.

I would also like to direct a big thank you to Jan Högberg and Daniel Asplund at the wind energy section of Dalakraft for answering all my questions and for providing vital information and data for the project work.

I also owe Johannes Hüffmeier, my brother in law, a whole bunch of thank yous for letting me use his computer during the simulations and for helping me out and explaining whenever I needed to understand issues concerning CFD simulation and flow modelling.

I would also like to thank WindSim AS for letting me use their software without charge during the time of the project.

Last but not least I would like thank all of you who have read and commented on the thesis, it has been very important.

Karl Nilsson
Visby 21/3-2010

Contents

List of Figures

List of Tables

Nomenclature and glossary

$N = kg\frac{m}{s^2}$ - Definition of the unit N (Newton) in SI units.

Roman letters	Description	Dimension	Value
a	Axial interference factor	$-$	$-$
a_{acc}	Acceleration	m/s^2	$-$
A, B	Stability coefficients	$-$	$-$
A_c	Cross section area	m^2	$-$
$A_{weibull}$	Weibull scale factor	m/s	$-$
c_1, c_2, c_μ	Constants	$-$	$-$
c_p	Heat capacity of air	Nm/K	$-$
C_p	Efficiency of wind turbine	$-$	$-$
$C_{p,max}$	Betz' limit	$-$	$16/27$
C_T	Thrust coefficient	$-$	$-$
E_∞	Energy content in free stream air	Nm	$-$
E_{kin}	Kinetic energy, $P_{kin}t$	Nm	$-$
E_o	Energy content in air behind rotor	Nm	$-$
E_r	Energy content in air at rotor	Nm	$-$
f	Coriolis parameter	rad/s	$-$
F_c	Coriolis force	N	$-$
F_{cent}	Centrifugal force	N	$-$
F_f	Friction force	N	$-$
F_g	Gravitational force	N	$-$
F_p	Pressure gradient force	N	$-$
g	Gravitational constant	m/s^2	$9,82$
h, z, z_a	Heights	m	$-$
H_0	Heat flux	N/ms	$-$
k	Turbulent kinetic energy	Nm	$-$
$k_{weibull}$	Weibull k shape factor	$-$	$-$
L	Monin-Obukhov length	m	$-$
m	Mass	kg	$-$
$\dot{m}$	Massflow of air	kg/s	$-$
$\dot{m}_\infty$	Massflow of free stream air	kg/s	$-$
$\dot{m}_o$	Massflow of air behind rotor	kg/s	$-$
$\dot{m}_w$	Massflow of in in wake	kg/s	$-$
p	Pressure	N/m^2	$-$
P_η	Porosity	$-$	$-$
P_{kin}	Kinetic power	Nm/s	$-$

P_{max}	Maximum power in streaming air	Nm/s	$-$
P_r	Output power of turbine	Nm/s	$-$
r	Radius	m	$-$
r_w	Radius of wake	m	$-$
r_o	Radius of air wake behind rotor	m	$-$
t	Time	s	$-$
$T, \Delta F$	Thrust force	N	$-$
T_0	Absolute temperature	K	$-$
u, u', u''	Wind velocities	m/s	$-$
u_*, u_{*1}, u_{*2}	Friction velocities	m/s	$-$
u_∞	Free stream air velocity	m/s	$-$
u_o	Air velocity behind rotor	m/s	$-$
u_r	Air velocity at rotor	m/s	$-$
u_w	Air velocity in wake	m/s	$-$
δu	Velocity decifit	$-$	$-$
x	Directional variable	m	$-$
z_0, z_{01}, z_{02}	Roughness lengths	m	$-$

Greek letters	Description	Dimension	Value
α	Wake expansion coefficient	$-$	$-$
ε	Turbulent dissipation rate	$Nm/(kgs)$	$-$
κ	von Karman's constant	$-$	0,40
ν	Kinetic viscosity	m^2/s	$-$
ν_T	Turbulent viscosity	m^2/s	$-$
ρ	Density of air	kg/m^3	1,225
φ	The latitude	$\circ$	$-$
ω	Earth's angular rotation speed	rad/s	

Glossary	Description
AEP	Annual Energy Production
CFD	Computational Fluid Dynamics
DK	Digitala Kartbiblioteket
$m.a.s.l.$	Meters above sea level
$Orography$	Height variation
$WAsP$	Wind Atlas Analysis and Application Program for wind energy simulations
$WindPRO$	Wind Atlas software
$WindSim$	Wind energy simulation software

Chapter 1

Introduction

1.1 Background

The narrow line between economic loss and economic success in wind power investments is partly dependent on how well the energy production is estimated before the construction of the wind farm. The most powerful tools used in the planning process are the wind simulation software which are extensively used within the wind energy business. There are different types of software which all have certain benefits and certain drawbacks in relation to different simulation parameters, e.g. landscape type, wind wake interaction etc. The accuracy of these software varies due to the different simulation parameters. It is therefore of interest to make an in-depth-study of the accuracy of these software in relation to the chosen simulation parameter. It is also of interest to study inherent limitations in the different software in order to determine which type of software that is suitable for a certain type of landscape and how the simulation should be performed.

In the report two different types of flow models will be used in the annual energy production simulations; linear and non-linear such as CFD. For wind energy simulations and calculations the linear models set the business standard today. The CFD technique has been used successfully in many businesses where fluid dynamics are important such as optimizing air flow over cars, water flow around boats etc. It has not, yet, been implemented in the flow dependent wind energy business on a large scale. Therefore it is of interest to study the outcome differences between linear and non-linear models used in wind power simulations. The different simulations will also give the opportunity to determine limitations within the different software.

1.2 Aim

The aim of this project work and report is to state differences in wind energy simulation for two software, employing different models, linear and non-linear, in their simulations. The main test parameter in the simulations is orographic complexity. Furthermore, by stating and analyzing the outcome differences this report will give a hint of when the different software, respectively, should be used in relation to variations of the test parameters.

1.3 Question formulation

When using a software based on a linear model, how well does the simulated wind energy production represent the measured production at high and low orographic complexity?

When using a software based on a non-linear model, how well does the simulated wind energy production represent the measured production at high and low orographic complexity?

At what grid resolution for the software based on a non-linear model does the simulated production converge for the different simulation situations?

1.4 Delimitations

This project work and report is delimited to study how orographic complexity affects energy production simulations of a linear simulation software, WAsP, and a non-linear software, WindSim which is using a CFD approach.

Two simulations sites have been chosen to study; Näsudden with a low orographic complexity and Hunnflen with a high orographic complexity. At Näsudden a wind turbine named Siral is chosen for the evaluation and at Hunnflen three turbines named Ferdinand, Vilhelm and Freja are chosen in the evaluation. The simulations and the outcome of this report are based on the analyze of the wind turbines on these simulation sites.

Other simulation parameters, e.g. wind turbine type, and simulation software might be described and mentioned briefly but will not be included in the simulations nor analyzed in depth.

1.5   Scientific methodology

The thesis constits of three main parts; the theoretical framework, the selection and analysis of appropriate simulation sites and the results.

The theoretical framework, which contains the theory about wind energy and flow models, is based on a literature study.

The selection and analysis of appropriate sites is based on the data, such as wind condition and type of wind turbine, given at each location. The location is selected according to the test parameter orographic complexity.

The results compare the simulation outcome for the different software and relates these outcomes to the theory presented in the theoretical framework.

1.6   Disposition

In this section, each chapter will be briefly decribed in terms of content, aim, importance and basis for study.

1.6.1   Chapter 2: Wind energy

The chapter covers a large area of knowledge and starts with how winds are approximated and ends with how the kinetic energy in the winds are converted into electrical energy by wind turbines. Aside from the areas above this section also describes measurement and visualization of wind energy content. Limitations in wind energy conversion and wind wakes will be described. This part is based on a literature study.

1.6.2   Chapter 3: Flow models

In the flow models chapter the basic theory behind each flow model will be described. Furthermore, some advantages and disadvantages of each flow model will be stated briefly.

1.6.3   Chapter 4: Methodology

The methodology chapter desicribes the simulation process in terms of input, simulations and output. The input is the terrain file prepared in WindPRO and the wind data used. The simulation is described in terms of how the simulation is conducted in each software. The output is how results are obtained and handled.

1.6.4 Chapter 5, 6, 7 and 8: Simulation sites, Results, Discussion and Conclusion

In the simulation sites chapter each simulation site will be analyzed and described. The results chapter displays the simulated results and the results is later discussed in relation to the theory in the discussion section and concluded in the conclusion section.

Chapter 2

Wind energy

This chapter presents how winds are approximated, measured, visualized and converted into electricity. It also presents two limitations of wind energy conversion, i.e. Betz' limit, which states that no more than 16/27 of the wind energy can be converted into electrical energy, and wind wakes, which is described in the wind wake section.

2.1 Approximations of winds

The air in the atmosphere is affected by various forces which are due to gravitation, rotation of the earth, sun radiation, ground friction and the movement of the air. Wind, i.e., moving air, is therefore dependent on these forces. This section will therefore start by stating and explaining these forces and end with putting these forces together in horizontal and vertical balances, [1].

2.1.1 Forces affecting wind

If we consider a small air parcel, there are different forces causing the parcel to move and thus creating wind. These forces will be described in this subsection.

Gravitational force The air parcel has a certain mass, m. This mass in combination with the gravitational constant, g defines the gravitational force according to equation 2.1. The force is directed downwards. Figure 2.1 presents the gravitational force.

$$F_g = mg \tag{2.1}$$
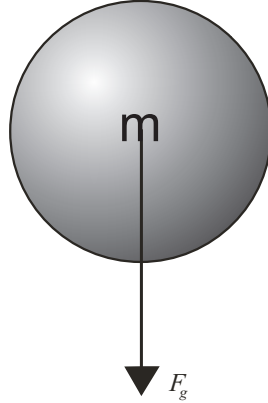
Figure 2.1: The circle represents an air parcel with mass m and the black arrow represents the gravitational force directed towards the ground.

Pressure gradient force   Since earth orbits the sun and in the same time rotates around its axis the sun radiation will not be equally distributed over the surface of the earth. The temperature will therefore differ around the globe since it is dependent on the energy per square meter due to sun radiation which in turn is dependent on the angle of which the sun rays hit the earth. For instant, if the sun rays hit the earth surface perpendicularly, the area where a certain amount of sun energy hits the surface is small in comparison, making the sun energy per square meter high and also the temperature. If the same amount of sun energy hits the surface but with a certain angle, the area will be smeared on a larger area and the sun energy per square meter will be low and thus leading to a low temperature, as shown in figure 2.2. Furthermore, the air in the atmosphere will therefore have different temperatures. When the air parcels are heated, they expand and high pressure areas are created. The high pressure air seeks equilibrium and moves towards low pressure areas. The pressure gradient force is a result of the pressure differences.

The pressure gradient force is defined according to equation 2.2.

$$F_p = -\frac{1}{\rho}\frac{\partial p}{\partial n} \tag{2.2}$$

where p is pressure, n is the normal to the isobars, and ρ the air density. The pressure gradient force is presented in figure 2.3.
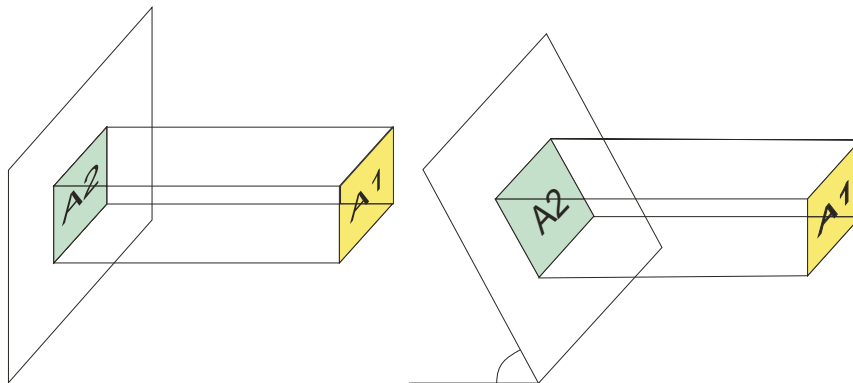
(a) Sun rays hit the surface perpendicularly and $A2 = A1$.

(b) Sun rays hit the surface with an angle and $A2 > A1$.

Figure 2.2: Sun ray smearing due to difference in hit angle.
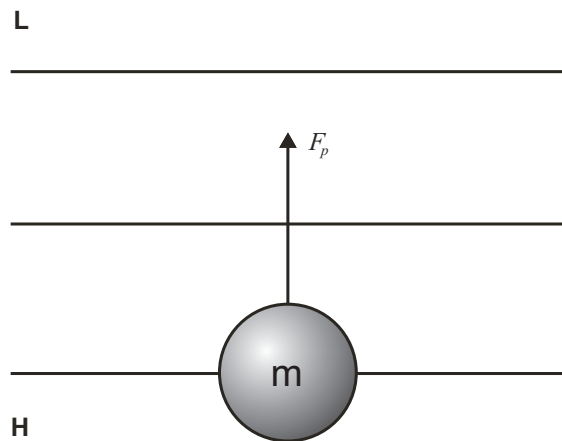
Figure 2.3: The circle represents an air parcel and the black arrow represents the pressure gradient force directed towards the low pressure area, L.

Coriolis force   The Coriolis force is due to the earths rotation and will cause the high pressure winds to move clockwise on the northern hemisphere and low pressure winds will move counter clockwise. The contrary applies for the southern hemisphere.

The Coriolis force is defined according to equation 2.3.

$$F_c = \pm f u \tag{2.3}$$

where u is the wind speed and $f = 2\omega \sin(\varphi)$. ω is the angular speed of

the earth's rotation and φ is the latitude.

Centrifugal force   When the air parcel suddenly change direction of movement it is affected by a force directed perpendiculary to the change of direction, as shown in figure 2.4.

The centrifugal force is defined according to equation 2.4.

$$F_{cent} = m\frac{u^2}{r} \tag{2.4}$$

where R is the radius of the direction change.
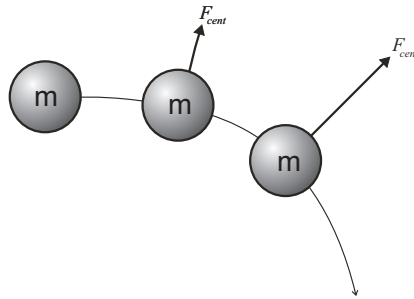
Figure 2.4: The circles represents an air parcel at different locations on its trajectory, the black arrow represents the centrifugal force affecting the air parcel.

Friction force   When air sweeps over the ground, friction appears. This friction in turn leads to a friction force directed in opposite direction to the wind direction. The friction force is dependent on wind speed and the so called roughness length which basically is a measure of how much the ground surface retards the wind speed at a certain location. A high roughness length retards the wind speed more than a low roughness lenth. Therefore, the friction force is higher in areas with high roughness length, e.g. dense forests, than in areas with low roughness length, e.g. open water. Roughness lengths are most often used in its classified version; the roughness class. The relationship between roughness length and class is presented in table 2.1. Figure 2.5 displays the friction force.

The friction force is defined according to equation 2.5.

$$F_f = -ku \tag{2.5}$$

where $k = f(z_0)$ and z_0 is the roughness length which is defined according to equation 2.6.

$$z_0 = ze^{-\frac{\kappa u}{u_*}} \qquad (2.6)$$

where z is the height, κ is von Karmans constant and u_* is the friction velocity.
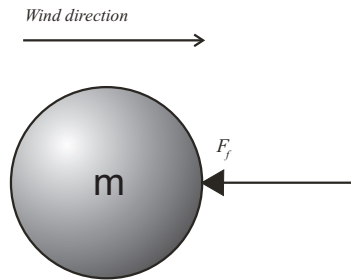
Figure 2.5: The circle represents an air parcel and the black arrow represents the friction force

Roughness class	Roughness length [m]	Type of landscape
0	$\leq 0{,}0002$	Open water
1	0,003	Open landscape
2	0,10	Partly open landscape
3	0,40	Smaller cities
4	1,60	Large cities or dense forests

Table 2.1: Relationship between roughness class, roughness length and landscape type

2.1.2 Putting forces together

The wind is moving in a three dimensional pattern. This pattern is influenced by the forces described above. The forces in turn exist either in the vertical direction or in the horizontal plane. The vertical direction and the horizontal plane accounts for the three dimensional space in where the wind moves. The section aims at identifying vertical and horizontal forces, respectively, and to balance these. This section is providing the hydrostatic balance in the vertical direction and three different balances for the horizontal plane.

Hydrostatic balance   There are mainly two forces acting on the air parcel in the vertical direction; the gravitational force and the vertical pressure gradient force. Therefore, these forces are equal at static equilibrium state which is called hydrostatic balance. In this case the air parcel is static why the centrifugal force, which is due to movements of the parcel, is disregarded. Equation 2.7 defines the hydrostatic balance.

$$F_g = F_p \tag{2.7}$$

Geostrophic balance   The geostrophic balance is a good approximation of wind direction and speed at a high altitude, normally at a height of 1000 m, [24]. This balance is used by both WAsP and WindSim as inputs in order to describe winds at high altitudes. A small air element is influenced by two forces according to the geostrophic balance; the coriolis force and the pressure gradient force. The pressure gradient force is always directed towards low pressure, and thus perpendicular to the isobars. The coriolis force is directed so that the wind moves clockwise according to figure 2.6. The so called geostrophic wind occurs when the the pressure gradient force and the coriolis force are equal. The wind is then traveling parallel to the isobars. The geostrophic wind is also unaffected by the friction of the ground, [1].
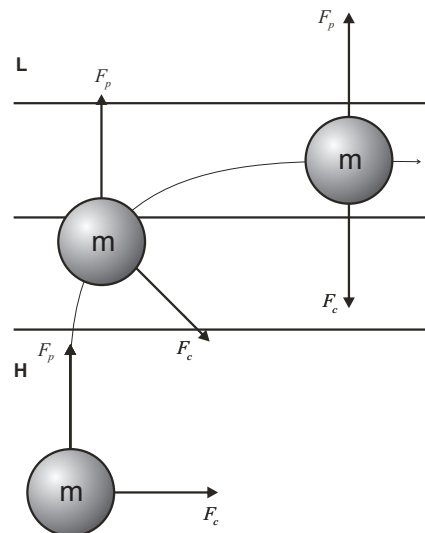
Figure 2.6: When the pressure gradient force is equal to the coriolis force, the geostrophic balance, the air will travel parallel to the isobars.

Gradient balance   The geostrophic balance requires that the wind blows in a straight line without change of direction. If this is not the case, as in most cases, the effects of the centrifugal force have to be taken into account. The centrifugal force will always be directed perpendicular to the change of direction as presented in figure 2.4.

Guldberg-Mohn balance   The Guldberg-Mohn balance applies for conditions close to the earths surface. This approximation is a revision of the geostrophic balance as it adds the friction force to the balance. The friction force will be in opposed direction to the wind and ill therefore slow the wind down. This will in turn make the coriolis force smaller since it is dependent on the wind speed. This results in a decreased wind speed and that the wind will cross the isobars at a certain angle, which is determined by the strength of the friction force and thus the roughness length of the surface, as the coriolis force is weakened.

The logarithmic velocity profile   The logarithmic velocity profile is basically an approximation of the vertical wind profile. It is independent of which of the balances above that are used and is described by the logarithmic velocity law, equation 2.8. Figure 2.7 shows the velocity log profile.

$$u = \frac{u_*}{\kappa} ln \frac{z}{z_0} \tag{2.8}$$

Figure 2.7: The logarithmic velocity profile.

2.2 Atmospheric stability

Atmospheric stability determines how well the atmosphere resists vertical movement of air parcels and is defined with the environmental lapse rate, where lapse rate is defined as the rate of temperature decrease due to increased elevation, and the so called adiabatic rate. The adiabatic rate is rate at which rate the air parcel cools and compresses or heats and decompress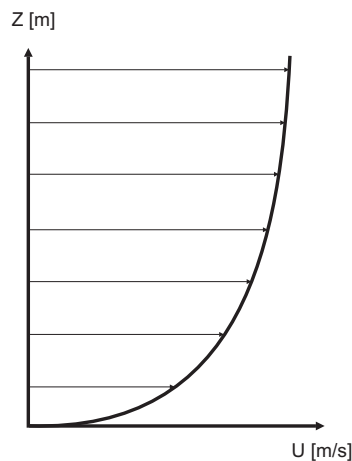es without interchanging heat with the surroundings. The dry adiabatic rate applies for unsaturated air and is more or less constant at 10 K cooling or warming per 1000 meter of change in elevation (cooling applies for increase in elevation and vice verse). The moist adiabatic rate applies for saturated air, when the air has a relative humidity of 100%. This rate is always lower than the dry adiabatic rate and is not constant as it varies with e.g. temperature, [2][4].

2.2.1 Absolute stable atmosphere

The atmosphere is absolute stable when the environmental lapse rate is lower than the moist adiabatic rate. For instance, if an air parcel in a stable atmosphere is elevated it will be cooled faster than the surroundings since its adiabatic cooling rate is higher than the environmental lapse rate. The air parcel will therefore be heavier than the surroundings and sink back to equilibrium state. The opposite applies when the air parcel is lowered. In this case the adiabatic heating rate is higher than the environmental lapse rate and thus resulting in that the air parcel is lighter than the surroundings. The air parcel will in this case rise back to equilibrium state, [2][4].

2.2.2 Neutral stable atmosphere

When the environmental lapse rate is equal to either the dry adiabatic rate at unsaturated conditions or the moist adiabatic rate at saturated conditions the atmosphere is neutral stable. This basically means that the air parcel will be heated or cooled with the same rate as its surroundings and thus have the same weight. The air parcel will in this case neither rise nor sink after perturbation, [2].

2.2.3 Absolute unstable atmosphere

The atmosphere is absolute unstable when the environmental lapse rate is higher than the dry adiabatic rate. In this case an elevated air parcel cools slower than the environmental lapse rate and is therefore warmer, and lighter,

than the surroundings. It rises further until an unstable equilibrium state is reached. A lowered air parcel continues sinking until unstable equilibrium is reached, [2][4].

2.2.4   Conditional stable atmosphere

When the environmental lapse rate lies between the dry and moist adiabatic rate, the atmosphere is conditionally stable. This means that when air is unsaturated the atmosphere is stable and when air is saturated the atmosphere is unstable, [2].

2.2.5   Variation over time

The atmospheric stability varies over time and is never constant at a certain location. At a site located on-shore the stability varies according to a 24 hour cycle, with a stable atmosphere during the night and a more unstable atmosphere during the day as shown in figure 2.8. The same cycle applies for off-shore conditions but is in this case over a longer period of time, which could be weeks or even months and is due to fact that water can "store" more energy than the ground, [16].
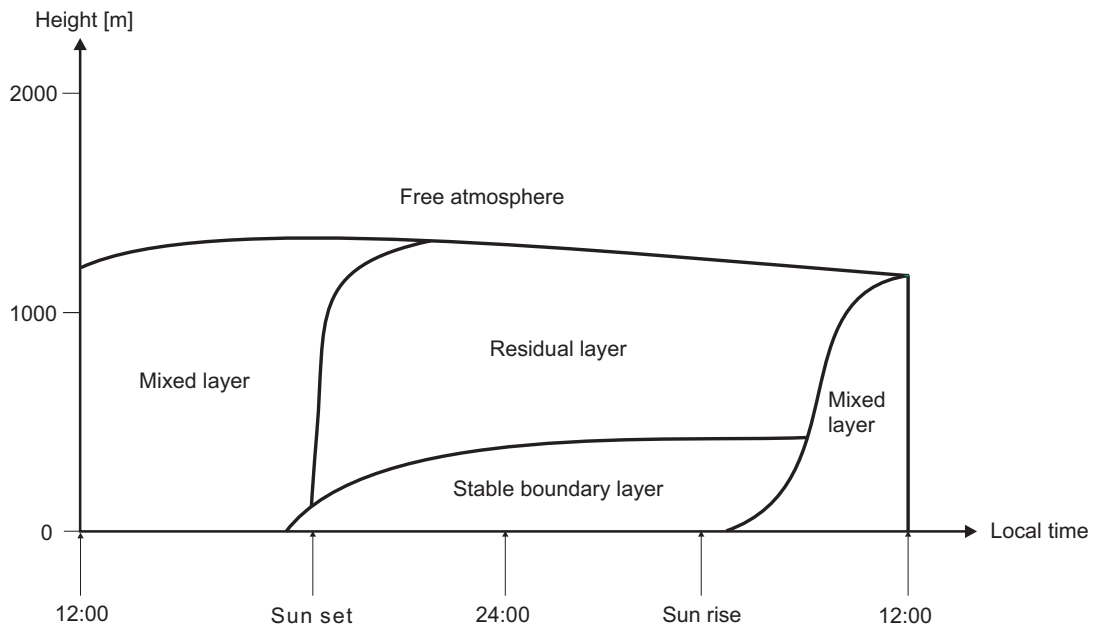

Figure 2.8: Changes of meteorological boundary layer during the day, [16].

13

2.3 Handling of wind data

In order to determine the wind conditions at a specific site one can measure the wind conditions directly on site or make a wind atlas calculation in order to transfer wind data from one site to another. This section describes different techniques in how to measure wind conditions, it describes how to calculate wind atlas data and it provides different ways of displaying wind energy content.

2.3.1 Measurement

The most accurate way of obtaining wind data is to simpy put a measuring device on the site. Measuring wind conditions on site gives you the possibility to register wind speeds and wind directions at different heights. These data can later be used to determine frequency distribution of the wind, energy content in the wind and the distribution of the wind direction. The result gets more accurate if the measuring takes place during a long period of time, [24]. Various techniques can be used for measuring wind data, such as traditional anemometers and more modern SODARs and LIDARs which are using sound and light, respectively, in the measurement.

2.3.2 Transfer

Measuring wind conditions is very time consuming. The so called wind atlas method offers a way to convert nearby located measuring points' data to the desired location, [24]. At location A a measuring mast has been collecting wind data for a satisfying period of time hence accurate profiles of wind frequency, direction and energy content have been established. The next step is to convert this data into wind atlas data. The wind data is dependent to the roughness class at the site. The data is recalculated to suit a roughness class of 1. This data is called the wind atlas data. The roughness class is determined at location B. The wind atlas data is again recalculated from roughness class 1 to the current roughness class of location B. Site B must be situated in a close radius to site A to get reliable results. Figure 2.9 shows the scheme of the wind atlas method.

2.3.3 Visualization

By using the wind atlas method, wind resource maps can be created, [24]. These maps give a rough view on how winds are distributed over land and sea. In Sweden, there are two types of wind resource maps; those who are
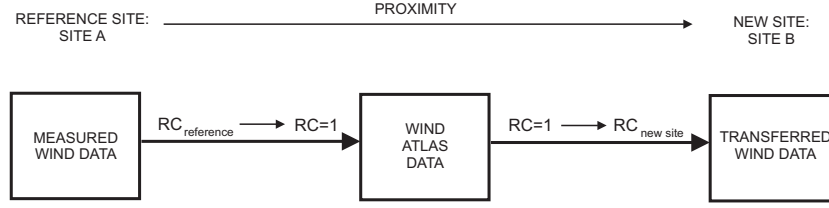
Figure 2.9: Wind atlas method.

displaying mean wind speeds and those who are displaying energy content per square meter. The relationship between mean wind speed and energy content per square meter is shown in equations 2.9 to 2.14.

Equation 2.9 describes the kinetic power in the wind.

$$P_{kin} = \frac{1}{2}\dot{m}u^2 \tag{2.9}$$

The massflow of wind is described according to equation 2.10.

$$\dot{m} = \rho A_c u \tag{2.10}$$

Equation 2.9 and 2.10 give,

$$P_{kin} = \frac{1}{2}\rho A_c u^3 \tag{2.11}$$

The energy in the wind is given according to equation 2.12 where the time is converted from seconds to hours by dividing t with 3600.

$$E_{kin} = P_{kin}t = \frac{1}{2}\rho A_c u^3 \frac{t}{3600} \tag{2.12}$$

In the next step the energy in the wind is converted in energy per square meter according to equation 2.13.

$$e_{kin} = \frac{E_{kin}}{A_c} = \frac{1}{2}\rho u^3 t \tag{2.13}$$

Number of hours per year, 8760, insterted in 2.13 give 2.14.

15

$$e_{kin,year} = \frac{1}{2}\rho u^3 8760 \qquad\qquad (2.14)$$

where P_{kin} is the power, $\dot{m}$ the massflow of air, u is mean wind speed, ρ is the density of air at the certain altitude, A_c is cross section area, E_{kin} is energy, e_{kin} is energy per square meter and t is the time. Figure 2.10 presents a wind resource map.

Figure 2.10: A wind resource map displaying mean wind speed over a part of Sweden, [3].

2.4 Conversion

The energy in the wind is converted into electricity by a wind turbine. In this section a typical wind turbine will be described briefly in terms of type of wind turbine and power control. These aspects affect the efficiency of the turbine aswell as the power curve. The efficiency and the power curve play important roles of the annual energy production of the turbine and is therefore included in this study.
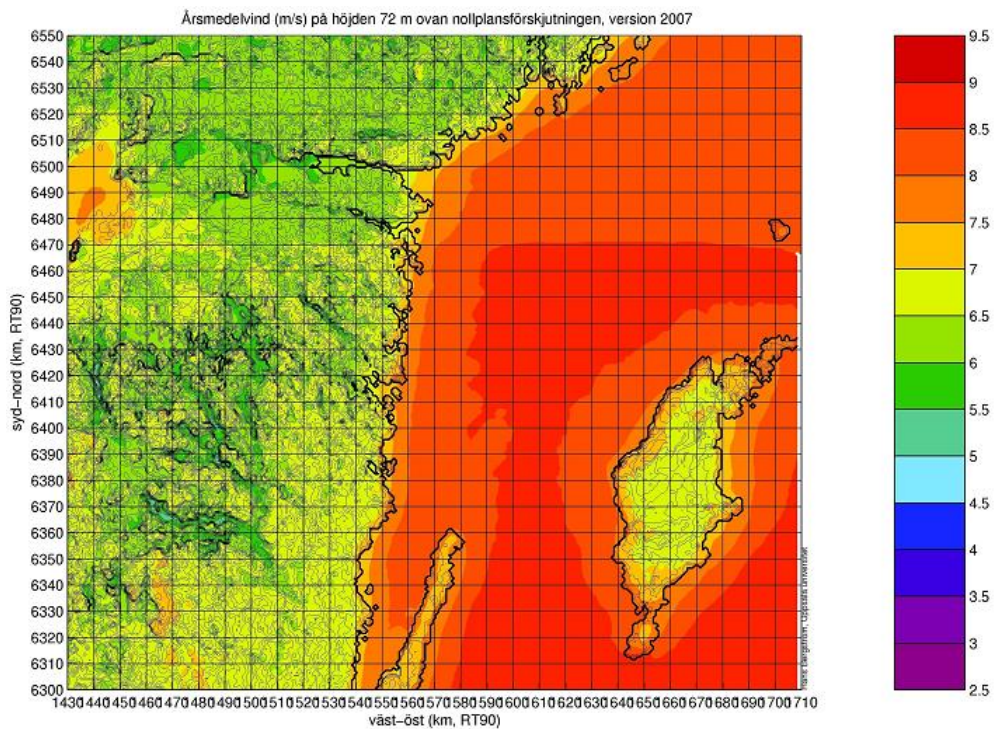
2.4.1 Power control

There are two different ways of controlling the power output of the wind turbine; pitch and stall regulation.

In order to decrease the power output with a pitch regulated turbine the blades pitches out of the wind in order to reduce the lift force and the rotation speed and thus the power output.

In the case of stall regulation, there are again two types; passive and active stall. In the case of passive stall, the rotor blades are bolted in a fix angle. When the wind speed reaches a certain amount, the momentum around the blades increases and the lift power decreases and so does the power output.

In the case of active stall, the rotor blades pitches into the wind in order to decrease the lift force and thus the power output, [19].

Figure 2.11 shows how the power curves vary for a wind turbine with passive stall regulation, NEG Micon 52, and a turbine with pitch regulation, Vestas V52.

2.5 Betz' limit

A wind turbine can never have an efficiency of 100% even when disregarding from operational losses. As shown below, the efficiency of the wind turbine can never exceed 16/27 or roughly 59% and this is called the Betz' limit, [10][24].

The first step when determining the Betz' limit is to make an energy balance over the control volume shown in figure 2.12 and thus declaring the energy over the rotor, as decribed by equation 2.15.

$$E_\infty = E_r + E_o \implies E_r = E_\infty - E_o \qquad (2.15)$$
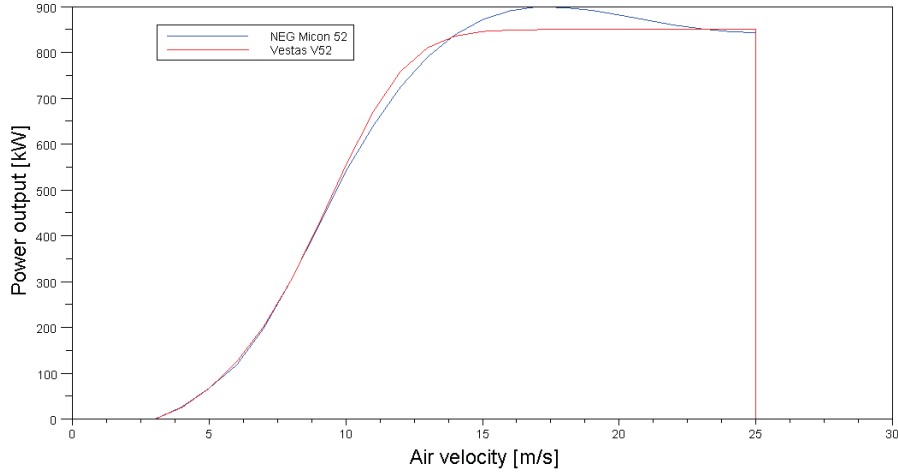
Figure 2.11: Stall and pitch power regulated wind turbines.
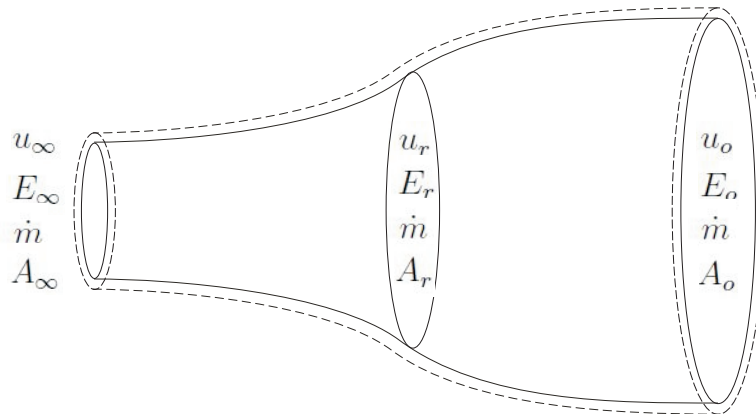
Figure 2.12: Control volume, [10].

Where E is energy, ∞ stands for free stream air, r stands for rotor and o stands for out, i.e., perpurbed air going out from the turbine.

Furthermore, the massflow is equal throughout the control volume, as described by equation 2.16.

$$\dot{m} = (\rho A_c u)_\infty = (\rho A_c u)_r = (\rho A_c u)_o \tag{2.16}$$

where $A_{c,\infty}$, $A_{c,r}$ and $A_{c,o}$ are cross sections areas shown in figure 2.12.

u_r can be calculated by using two different formulas describing the power over the rotor. First, the power is described by making a balance of forces around the rotor, as described by equation 2.17.

$$dF = dma_{acc} = dm\frac{du}{dt} = \dot{m}du \implies \Delta F = \dot{m}\Delta u \qquad (2.17)$$

where dF is force acting on the air parcel with the weight dm. a_{acc} is the acceleration of the air parcel and ΔF is the change of force which is equal to the trust force T according to 2.18.

$$\Delta F = T \qquad (2.18)$$

The change of air velocity is equal to the difference between the velocity at the inlet and the velocity at the outlet according to equation 2.19.

$$\Delta u = (u_\infty - u_o) \qquad (2.19)$$

Equation 2.17, 2.18 and 2.19 redefine T and give,

$$T = \dot{m}(u_\infty - u_o) \qquad (2.20)$$

The output power of the turbine is defined in equation 2.21.

$$P_r = \frac{dE_r}{dt} = \frac{Tdx}{dt} = Tu_r \qquad (2.21)$$

Equation 2.16, 2.20 and 2.21 give

$$P_r = (\rho A_c u^2)_r (u_\infty - u_o) \qquad (2.22)$$

The same power can be described by using kinetic energy, $E = \frac{1}{2}mu^2$ and equation 2.15 give,

$$E_r = \tfrac{1}{2}m(u_\infty^2 - u_o^2)$$

using the differential equation according to equation 2.23 gives,

$$\implies dE_r = \frac{1}{2}dm(u_\infty^2 - u_o^2) \qquad (2.23)$$

Equation 2.21 and 2.23 give,

$$P_r = \frac{dE_r}{dt} = \tfrac{1}{2}dm(u_\infty^2 - u_o^2)\tfrac{1}{dt} =$$

$$= \frac{1}{2}\dot{m}(u_\infty^2 - u_o^2) = \frac{1}{2}(\rho A_c u)_r (u_\infty^2 - u_o^2) \tag{2.24}$$

Equation 2.22 equals equation 2.24 which gives equation 2.25,

$$(\rho A_c u^2)_r (u_\infty - u_o) = \frac{1}{2}(\rho A_c u)_r (u_\infty^2 - u_o^2) \tag{2.25}$$

In which u_r can be determined as a function of u_∞ and u_o

$$u_r = \frac{1}{2}(u_\infty + u_o) \tag{2.26}$$

At this stage parameter a is introduced. a is the axial interference factor and is a measure of the air velocity decifit over the turbine.

$$a = \frac{u_\infty - u_r}{u_\infty} \tag{2.27}$$

Equation 2.27 gives,

$$u_r = u_\infty(1 - a) \tag{2.28}$$

Equation 2.26 and 2.28 give,

$$u_o = u_\infty(1 - 2a) \tag{2.29}$$

Equation 2.24, 2.28 and 2.29 give,

$$P_r = \frac{1}{2}(\rho A_c)_r u_\infty^3 [4a(1 - a)^2] \tag{2.30}$$

$$P_{max} = \frac{1}{2}(\rho A_c)_r u_\infty^3 \tag{2.31}$$

Equation 2.30 and 2.31 give,

$$C_p = \frac{P_r}{P_{max}} = 4a(1-a)^2 \tag{2.32}$$

To calculate a maximum of C_p for a certain a we put $\frac{dC_p}{da} = 0$
$C_{p_{max}} = \frac{16}{27}$ for $a = \frac{1}{3}$ and this is called Betz' limit.

Betz' limit states that the efficiency of a single wind turbine can never exceed approximately 59%. This is hereby defined as the aerodynamic efficiency. In operation, there are also other types of losses in a wind turbine, e.g. friction losses which will reduce the turbine efficiency further, [24].

2.6 Wind wakes

When determining Betz limit we stated that a wind turbine can only use about 59% of the wind energy according to the previous section. This is achieved when the free stream air velocity is retarded with 2/3. The free stream air velocity behind the turbine is therefore only 1/3 of the velocity in front the turbine. Since the wind energy is dependent of the wind velocity, the wind contains less energy after the turbine than in front of. This phenomenon is referred to as wind wakes and when wakes from many turbines interact it is called wind wake interaction. To minimize the effect of wind wake interaction, turbines are normally placed in a certain pattern in relation to the predominant wind direction. The wind wake interaction will decrease the production of wind farms depending on the size of the farm. For a farm of 5-10 turbines a decrease of approximately 5% in production can be expected, [24].

Wake effects will only be looked at in Simulation B, the high orographic complexity simulation at Hunnflen. To get comparable results, a wake model which is used in both WAsP and in WindSim is chosen. The N.O. Jensen model, see section 2.5.1, is chosen as it can be used in both software. There are numerous other wake models but due to time constraints and software limitations these have not been used in the simulations.

Before describing the wind wake model that will be used, the thrust coefficient, C_T has to be declared since it plays an important role in the model. Furthermore, the wind wake model will be described in section 3.3.

Equation 2.21 and 2.24 give the thrust force,

$$T = \frac{1}{2}(\rho A_c)_r(u_\infty^2 - u_o^2) \tag{2.33}$$

Equation 2.29 and 2.33 give,

$$T = \frac{1}{2}(\rho A_c)_r u_\infty^2 [4a(1-a)] \tag{2.34}$$

The thrust coefficient is then defined according to equation 2.35.

$$C_T = \frac{T(a)}{T(a = \frac{1}{2})} = 4a(1-a) \tag{2.35}$$

2.6.1 N.O. Jensen wake model

This model is based on momentum deficit theory where the wake radius is assumed to expand linearly, [11]. The velocity deficit is described further below and figure 2.13 presents the linear expansion of the wake.

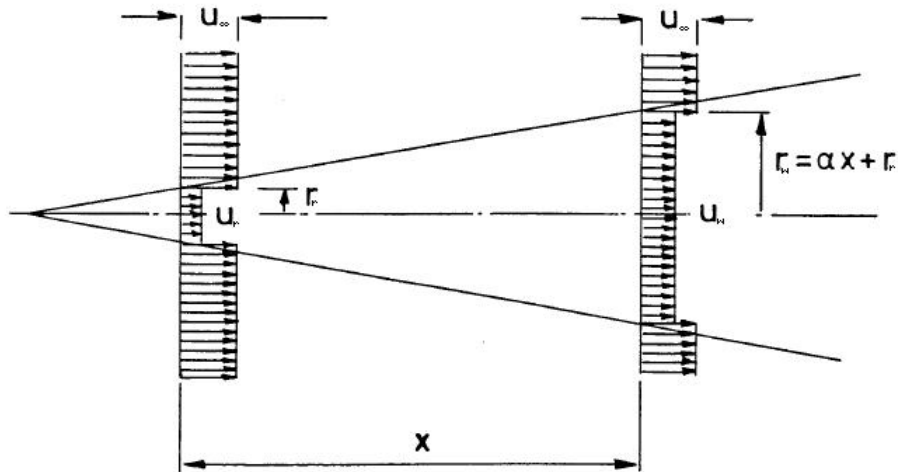
Figure 2.13: Principle scetch over the linear wake expansion according to N.O. Jensen, [11].

Looking at a cross section of the flow at a distance x from the turbine, the model assume that the massflow in this point is equal to the massflow

for the free stream air plus the massflow for the stream through the turbine at the distance $x = 0$ according to equation 2.36.

$$\dot{m}_w(x) = \dot{m}_\infty + \dot{m}_o \implies \rho A_{c,w}(x)u_w(x) = \rho A_{c,\infty}u_\infty + \rho A_{c,o}u_o \qquad (2.36)$$

where $A_{c,w} = \pi r_w^2$ is the circular cross section area of the wake at the distance x from the turbine and where r_w is the radius, $A_{c,o} = \pi r_o^2$ is the circular cross section area of the turbine rotor, where r_o is the radius and $A_{c,\infty} = \pi(r_w^2 - r_o^2)$ is the circular cross section area of the free stream air at the turbine. u_w is the wind velocity at the distance x behind the turbine.

the expressions o f the cross section areas and equation 2.36 give,

$$\pi r_w^2 u_w = \pi(r_w^2 - r_o^2)u_\infty + \pi r_o^2 u_o \qquad (2.37)$$

Equation 2.29 and 2.37 define the wind velocity at the distance of x behind the turbine according to equation 2.38.

$$u_w = \frac{(r_w^2 - r_o^2)}{r_w^2}u_\infty + \left(\frac{r_o}{r_w}\right)^2 (1 - 2a)u_\infty \qquad (2.38)$$

Simplification of equation 2.38 give equation 2.39.

$$1 - \frac{u_w}{u_\infty} = 2a\left(\frac{r_o}{r_w}\right)^2 \qquad (2.39)$$

where $1 - \frac{u_w}{u_\infty} = \delta u(x)$ which is the velocity decifite at the distance x behind the turbine.

Equation 2.40 to will relate the velocity decifite to the thrust coefficient, C_T.

Equation 2.35 gives,

$$a = \frac{1}{2}(1 - \sqrt{1 - C_T}) \qquad (2.40)$$

The radius is linearly proportional to the distance x which gives equation 2.41.

$$r_w = r_o + \alpha x \implies \left(\frac{r_o}{r_w}\right)^2 = \frac{1}{\left(1 + \alpha\frac{x}{r_o}\right)^2} \qquad (2.41)$$

Equation 2.39, 2.40 and 2.41 give equation 2.42 which describes the wind speed decifit behind the turbine in relation to C_T according to the N.O. Jensen wind wake model.

$$\delta U = \frac{1 - \sqrt{1 - C_T}}{\left(1 + \alpha \frac{x}{r_o}\right)^2} \qquad (2.42)$$

Chapter 3

Software

Three software are used during the simulation process. WindPRO is used in the preparation part and WAsP and WindSim are used in the simulation part.

The choice of using WindPRO is made due to previous experience with the software. This saves time in the project process. A full version of WindPRO was available during the project.

WAsP can be used either as a standalone program or in the WindPRO interface. For this project work WAsP is used in the WindPRO interface. This choice is made due to previous experience with this combination. A full version of WAsP was available during the project.

Prior to this project, the author had no experience with WindSim. However, WindSim is the only commercial software based on the non-linear model which was easily available during the project. A full version of the software was available during the project.

There are other software which can be used for the same purposes as those in this project work. However, due to time constraints and availability, these software have been neglected.

3.1 WAsP

WAsP, Wind Atlas Analysis and Application Program, is a wind simulation software based on the linear model described in section 3.1. The software was initially developed in the 80s Risø National Laboratory in Roskilde, Denmark, [17]. Risø National Laboratory merged with the Technical University of Denmark, DTU, in 2007 and is now known as Risø DTU National Laboratory for Sustainable Energy, [14]. WAsP is today developed and distributed by the wind energy division at Risø DTU and has more than 2900 users

worldwide, [15].

WAsP can be used for various purposes such as:

- estimating and optimising wind farm production and efficiency,

- mapping of wind resources,

- digitilising information on maps, such as height contours.

3.2 WindSim

WindSim is a CFD wind simulation software based on the non-linear model described in section 3.2. The software was initially developed in the beginning of the 21st century by Vector AS in Tønsberg, Norway. In 1998 Vector AS conducted an inventory of the wind conditions along the complex coastline of Norway in cooperation with the Norwegian Meteorological institute and this was when the idea of WindSim was born. A UNIX beta version was launched in 2003 and the first commercial Windows based version was launched in 2005. This was also when the company changed its name from Vector AS to WindSim AS, [21]. Today WindSim has more than 150 licensed users, [23].

The software can be used for various purposes such as:

- estimating and optimising wind farm production and efficiency,

- mapping of wind resources.

The software is especially useful if the site has complex orography and/or complex climatology, [22]. However, the software lacks the opportunity to digitilise maps and hence relies on third party software such as WindPRO and WAsP.

3.3 WindPRO

WindPRO is a software used for designing and planning for single wind turbines and wind farms. The software has been developed for more than 20 years by EMD International A/S in Aalborg, Denmark. The software has a modular structure which means that only the needed modules have to be chosen and be paid for. For instance, WindPRO can calculate noise generation caused by wind farms and a planner who works only with this issue only needs the DECIBEL (Noise) module. The sofware is available in

many languages and is based on a user-friendly map and coordinate system, [6] [7].

The software can be used for various purposes such as:

- digitilising information on maps, such as height contours,

- simple energy estimations of single wind turbines and wind farms,

- calculate generation of noise and shadows,

- make photo montages of the landscape with wind turbines.

Chapter 4

Flow models

In this chapter the different flow models used in the different simulations will be presented.

4.1 Linear model

In this section the linear model used in WAsP will be presented. Originally, the WAsP model was described in Troen and Petersen (1989) and this section is based on this book, [17]. WAsP uses the wind atlas model (not to be confused with the wind atlas method) which is a linear model combining a physical model (e.g. atmospheric stability, roughness changes, shelters and landscape orography) and a statistical model, i.e., Weibull distribution of the wind, in the analysis.

For further details it is referred to Troen and Petersen (1989).

4.1.1 Physical model

Equation 4.1 and 4.2 are used in WAsP in order to describe the surface layer wind profile. This is needed when transforming a wind speed at a certain height to a wind speed at another height.

$$u(z) = \frac{u_*}{\kappa} ln \frac{z}{z_0} \tag{4.1}$$

Where $u(z)$ is the air velocity at a height of z, u_* is the air friction velocity, κ is von Karmans constant which in this case is set equal to 0,40 and z_0 is the roughness length of the surface.

$$u(z) = \frac{u_*}{\kappa}\left(ln\frac{z}{z_0} - \psi(\frac{z}{L})\right) \tag{4.2}$$

Equation 4.1 applies for high wind speeds over a homogenous terrain and is refered to as the logarithmic wind law, see figure 2.7. Equation 4.2 includes an empirical stability function, $\psi(\frac{z}{L})$, in order to compensate for lower wind speeds and surface heat flux. L is the Monin-Obukhov length which is defined according to equation 4.3.

$$L = \frac{T_0}{\kappa g}\frac{c_p u_*^3}{H_0} \tag{4.3}$$

Where T_0 and H_0 are the absolute temperature and heat flux, respectively. c_p is the heat capacity of air at constant pressure and g is the gravitation constant.

The geostrophic wind is incorporated by WAsP in the geostrophic drag law, equation 4.4, which is a balance between the friction velocity and the geostrophic wind.

$$G = \frac{u_*}{\kappa}\sqrt{\left(ln(\frac{u_*}{fz_0}) - A(\mu)\right) + B(\mu)^2} \tag{4.4}$$

A and B parameters are at neutral stability conditions constants but at non-neutral stability conditions they are function of μ, the atmospheric stability parameter which is described in equation 4.5.

$$\mu = \frac{\kappa u_*}{fL} \tag{4.5}$$

Stability submodel   This model describes the stability of the atmosphere. It is derived from the geostrophic drag law and accounts for variations in surface heat flux which in turn will have an impact on the wind profile. Instead of treating each variation of the surface heat flux and its impact on the wind profile, the model uses the root-mean-square of the heat flux. Among other equations the empirical stability equation, equation 4.6, is derived and described for stable and unstable conditions.

$$\psi(\frac{z}{L}) = \begin{cases} -4.7\frac{z}{L} & \text{if conditions are stable} \\ \left(1 - 16\frac{z}{L}\right)^{1/4} - 1 & \text{if conditions are unstable} \end{cases} \qquad (4.6)$$

Roughness change submodel The logarithmic wind profile is valid only for homogenous terrain conditions. If the roughness of the terrain changes, the logarithmic wind profile has to be compensated in order to cover for these changes. When there is a change of roughness, the height of the internal boundary layer will change. The wind profile above the boundary layer before the change will be unaffected but the wind profile below will change, as shown in figure 4.1.
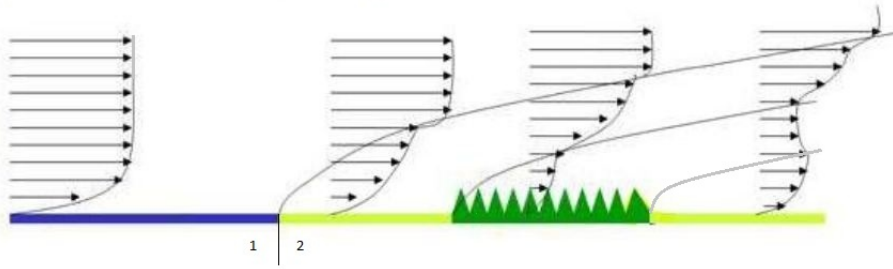
Figure 4.1: The change of wind profile due to roughness change.

Equation 4.7 has empirically been established between the friction velocity before, u_{*1}, and after, u_{*2}, the change and the roughness length before, z_{01}, and after, z_{02} the change.

$$\frac{u_{*2}}{u_{*1}} = \frac{ln(h/z_{01})}{ln(h/z_{02})} \qquad (4.7)$$

Where h is the height of the internal boundary layer.

The perturbed wind profile is divided into three parts by the submodel and is described by equation 4.8.

$$u(z) = \begin{cases} u' \frac{ln(z/z_{01})}{ln(c_1 h/z_{01})} & \text{for } z \geq c_1 h \\ u'' + (u' - u'') \frac{ln(z/c_2 h)}{ln(c_1/c_2)} & \text{for } c_2 h \leq z \leq c_1 h \\ u'' \frac{ln(z/z_{02})}{ln(c_2 h/z_{02})} & \text{for } z \leq c_2 h \end{cases} \qquad (4.8)$$

Where $u' = \frac{u_{*1}}{\kappa} ln \frac{c_1 h}{z_{01}}$, $u'' = \frac{u_{*2}}{\kappa} ln \frac{c_2 h}{z_{02}}$, $c_1 = 0.3$ and $c_2 = 0.09$.

Shelter submodel   The wind profile at the site of the turbine is affected by all obstacles close to the turbines. Obstacles in a general view are everything ranging from individual sand grains and leaves to large trees and buildings. Most of these obstacles are however already described by the roughness length and are not covered in the shelter model. The shelter model corrects the wind profile for deviations due to large single obstacles such as buildings. After the obstacle a wind wake will emerge. The size of the wake is mainly affected by the size and porosity of the obstacle. The wind wake leads to a decrease in wind speed behind the obstacle. The decrease is derived empirically and can be defined as equation 4.9.

$$\frac{\Delta u}{u} = 9.8 \left(\frac{z_a}{h}\right)^{0.14} \frac{x}{h} (1 - P_{eta}) \eta exp(-0.67 \eta^{1.5}) \qquad (4.9)$$

Where $\frac{\Delta u}{u}$ describes the decrease in wind speed, P_{eta} the porosity, h the height of the obstacle, z_a the considered height and x the downstream distance. η is defined according to equation 4.10.

$$\eta = \frac{z_a}{h} \left(\frac{0.32}{ln(h/z_0)} \frac{x}{h}\right)^{-0.47} \qquad (4.10)$$

Orographic submodel   The orography model corrects the measured wind data to correspond to height variations around the wind mast and the wind turbine. The model uses a horizontal grid which expands radially from the site of the turbine and the wind measuring point and uses polar representation, as shown in figure 4.2. The resolution is higher closer to the points of interest and decreases with factor to 1.06 radially. This allows a very high resolution close to the point of interest.
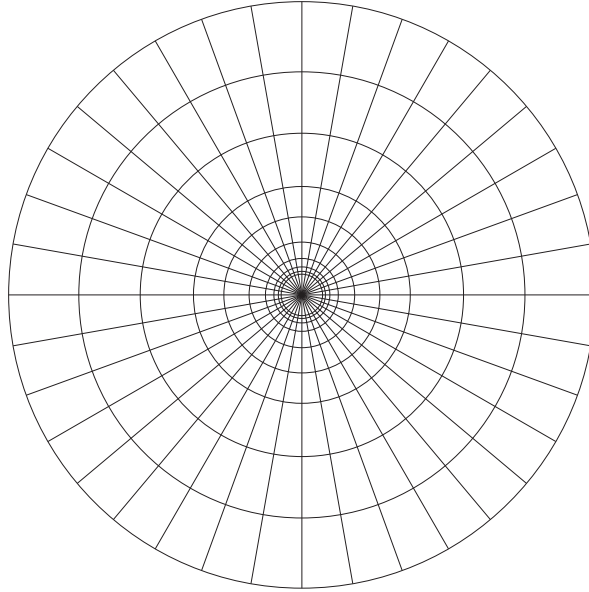
Figure 4.2: The radial grid.

4.1.2 Statistical model

The statistical model supplies a frequency distribution of wind speeds and wind directions for the different sectors in the area and is described by equation 4.11 which is know as the two-parameter Weibull distribution.

$$f(u) = \frac{k_{weibull}}{A_{weibull}} \left(\frac{u}{A_{weibull}} \right)^{k_{weibull}-1} exp \left(- \left(\frac{u}{A_{weibull}} \right)^{k_{weibull}} \right) \qquad (4.11)$$

Where $k_{weibull}$ is the shape parameter and $A_{weibull}$ is the scale parameter. Figure 4.3 shows an example of a weibull distribution plot.

Figure 4.3: Weibull distribution plot for scale A = 8 and shape k = 2.

4.2 Non-linear model

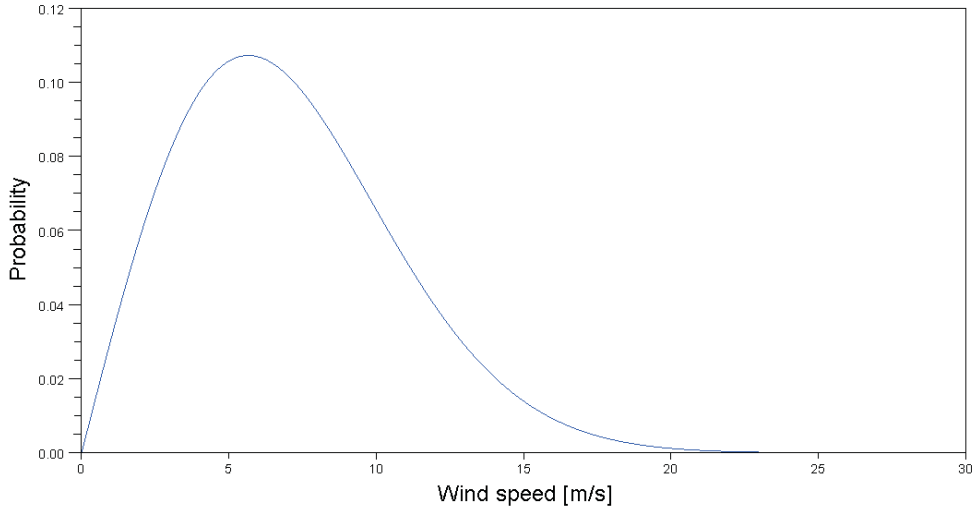The non-linear model used in WindSim is a CFD model based on Reynolds Averaged Navier-Stokes (RANS) equations with k-epsilon, or a modified version, turbulence model, [8]. The equations are non-linear, partial differential equations which in turn mean that the model is iterative, i.e., the results are numerically determined. Navier-Stokes equations apply for continuous substances and stem from the equations of conservation of mass, momentum and energy for a control volume, [20]. RANS uses simplified versions of Navier-Stokes equations and in order to account for turbulence in the calculations, a turbulence model is required, otherwise the number of unknown variables will be greater than the number of equations.

There are six flow variables that are solved in the iteration process; pressure, three velocity components, turbulent kinetic energy and turbulent dissipation rate. Each variable needs to be solved to reach a converged solution, see appendix A.2.1 for curves of convergence for flow variables.

4.2.1 The 3-dimensional model

The 3-dimensional model that is used has a predefined ground structure, length, width and height. The model is then divided into a predefined number

34

of 3-dimensional cells. The six flow variables described above is computed for each cell in the model. A rough representation of the model is presented in figure 4.4.
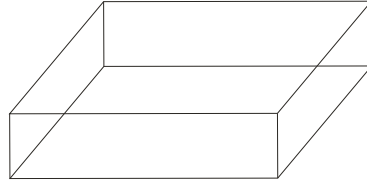

Figure 4.4: A rough representation of the 3-dimensional terrain model.

4.2.2　Boundary conditions

In WindSim the flow calculations start with initial boundary conditions and iterate until convergence is reached. Different boundary conditions are applied depending on the boundary. Alongside the vertical border of the 3-dimensional model, shown in figure 4.5, the same logarithmic wind profile as described in the wind energy and linear model sections, equations 2.8 and 4.1 is imposed. Profiles of k and ε, which are used in the turbulence model, are also imposed at the borders. At the ground, figure 4.6, wall functions are used through which no air can pass and at the top, figure 4.7, there are two ways of declaring the boundary conditions; it can either be set as a no friction wall through which no air can pass or as fixed pressure, which generates a plane with a homogenous pressure at the chosen height. Above the top boundary layer, the geostrophic balance, see section 2.1.2, is applied with a certain wind speed which is considered as constant. The atmospheric stability, see section 2.2, can altered by the use of potential temperature depending on the site and situation.
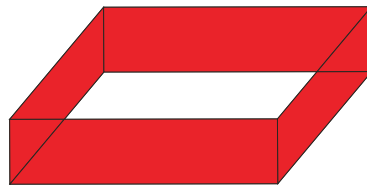

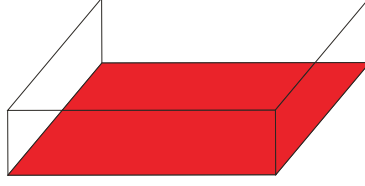**Figure 4.5:** The borders of the 3-dimensional model.

Figure 4.6: The ground of the 3-dimensional model.
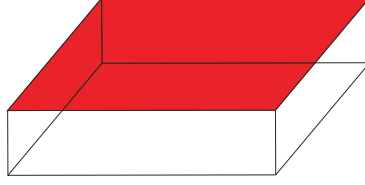
Figure 4.7: The top of the 3-dimensional model.

4.2.3 Governing equations

In this subsection one can find the governing Navier-Stokes equations used in the non-linear model.

Equation 4.12 describes the mass conservation which is assumed to be equal to 0.

$$\frac{\partial u_i}{\partial x_i} = 0 \tag{4.12}$$

Equation 4.13 describes the momentum conservation.

$$u_j \frac{\partial u_i}{\partial x_j} = -\frac{1}{\rho}\frac{\partial p}{\partial x_i} + \frac{\partial}{\partial x_j}\left(\nu\left(\frac{\partial u_i}{\partial x_j} + \frac{\partial u_j}{\partial x_i}\right) - (\overline{u_i u_j})\right) \tag{4.13}$$

where u is velocitiy, x is the positional component, p is pressure and ν is the kinetic viscosity. $\overline{u_i u_j}$ is the turbulence closure which is determined according to equation 4.14.

$$(\overline{u_i u_j}) = -\nu_T\left(\frac{\partial u_i}{\partial x_j} + \frac{\partial u_j}{\partial x_i}\right) + \frac{2}{3}\delta_{ij}k \tag{4.14}$$

where ν_T is the turbulent viscosity and k is the turbulent kinetic energy. ν_T is defined according to equation 4.15.

$$\nu_T = c_\mu \frac{k^2}{\varepsilon} \tag{4.15}$$

where c_μ is a turbulence model constant and ε is the turbulent dissipation rate.

For further details it is referred to Gravdahl (1998).

4.2.4 Statistical model

There are two ways the non-linear model can handle statistical wind data. Either as time series during certain period of time or as frequency tables. Time series are basically wind speeds and directions that are measured in a certain time interval, e.g. every 10 minutes, and thus giving a rather exact picture of the wind conditions at the site. Frequency tables display wind speeds and directions in summarized tables. Since time series files tend to become very large when the measuring time is long, frequency tables are suitable in this case.

4.3 Differences in models

Imagine a wind measuring device placed on top of a hill. If the hill slope is less than approximately 17° or 30%, the wind will accelerate up the hill and the measuring device on the hill will register a high wind speed. If the slope is larger than 17°, wind separation occurs, as shown in figure 4.8, and the registered wind speed is low. The major difference between the two software in this aspects is how they treat this separation.
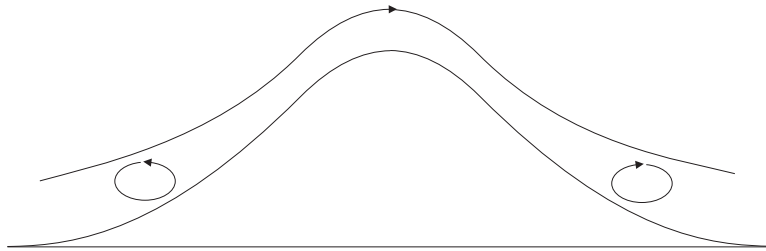

Figure 4.8: Wind separation due to high angle slope, [20].

The linear approach cannot account for this separation and treats the flow as attached over the hill, as shown in figure 4.9. This basically leads to
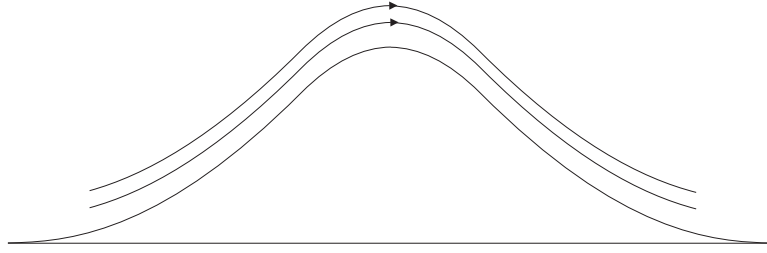
Figure 4.9: The attached wind in linear model, [20].

an overestimation of wind speed prediction for hills with a larger slope than 17°.

The non-linear model, however, can account for this separation due to the use of the turbulence model. The accuracy of the wind speed prediction is therefore high even for slopes that exceed 17°, [20].

Energy is proportional to the wind speed to the power of three, equation 4.16.

$$E_{kin} = ku^3 \tag{4.16}$$

The energy for the wind speed of 10 m/s is determined by equation 4.17.

$$E_{kin}(u = 10) = k10^3 = k1000 \tag{4.17}$$

If the wind speed is predicted as 10% too high, i.e., totally 11 m/s, the energy is determined by equation 4.18.

$$E_{kin}(u = 11) = k11^3 = k1331 \tag{4.18}$$

The percental increase of energy due to the over estimation of wind speed is described in equation 4.19

$$\frac{E_{kin}(u = 11) - E_{kin}(u = 10)}{E_{kin}(u = 10)} * 100 = 33,1\% \tag{4.19}$$

Chapter 5

Methodology

This chapter describes how the simulation process is executed. Figure 5.1 provides an overview over the logical sequence of the simulation process, from preparation to simulation.
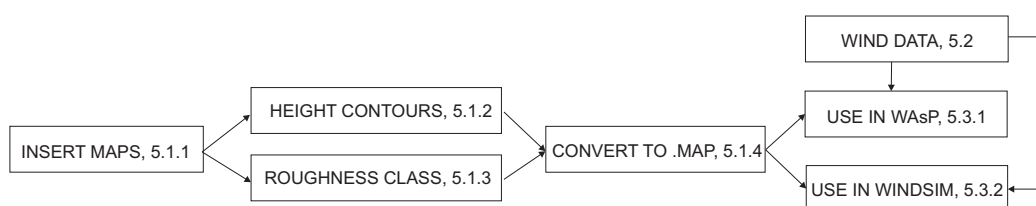
Figure 5.1: The simulation process.

5.1 Terrain file

This section describes how the terrain file is created in WindPRO. WindPRO is used as the basis for the simulation in both WAsP and WindSim. Hence, the first section applies for both WAsP and WindSim. Screenshots of each software are found in appendix A.

5.1.1 Maps

A set of maps is used as the basis for this purpose. The maps are downloaded from Digitala kartbiblioteket (DK). Digitala kartbiblioteket offers maps of high resolution which can be downloaded for free by students. The following map scales are used in order to get a detailed aswell as overall views of the site and the nearby located terrain.

- scale 1:12,500,

- scale 1:50,000 ,

- scale 1:100,000.

When downloading three different sets of X and Y coordinates have to be used for each map. The coordinates should create a triangular area on each map and this area should be as large as possible. In WindPRO these real coordinates is related to pixel coordinates on the map and the map is placed with a high accuracy on the world map.

Drawing of circles When the set of maps is correctly placed the next step is to locate the site for the wind turbine which can be done if real coordinates of the wind turbine are known. After pointing out the location, it is practical to draw two circles with the centers exactly at the locations of the turbine and the measuring mast in order to facilitate for the roughness classification near the sites. The circles should have a diameter of 4,000-6,000 m. The reason to the chosen distances and why circles are used is firstly that the area closest to the wind turbine (i.e. 2,000-3,000 meter) is especially important to examine closely . For this purpose the onsite observations and the 1:12,500 scaled maps are used. The area outside circles is examined by using the 1:50,000 scaled map and is therefore less accurate. For areas not covered by the 1:12,500 and 1:50,000 scaled maps, the 1:100,000 scaled map is used. Figure 5.2 and figure 5.3 show maps over näsudden and Hunnflen with the drawn circles included.

5.1.2 Height contours

In both WAsP and WindSim simulations the landscape complexity is described by height contours handled in WindPRO. These height contours are downloaded from DK in shape format. The height contours found at DK have no associated heights. In WindPRO each height contour has therefore been manually associated with a height.

5.1.3 Roughness class

There are three ways of doing the roughness classification in WindPRO. Firstly, a so called wind rose can be made. By using this method the area around the wind turbine is divided into 12 equally sized sectors. Each sector is then carefully examined by the user in order to discover changes in
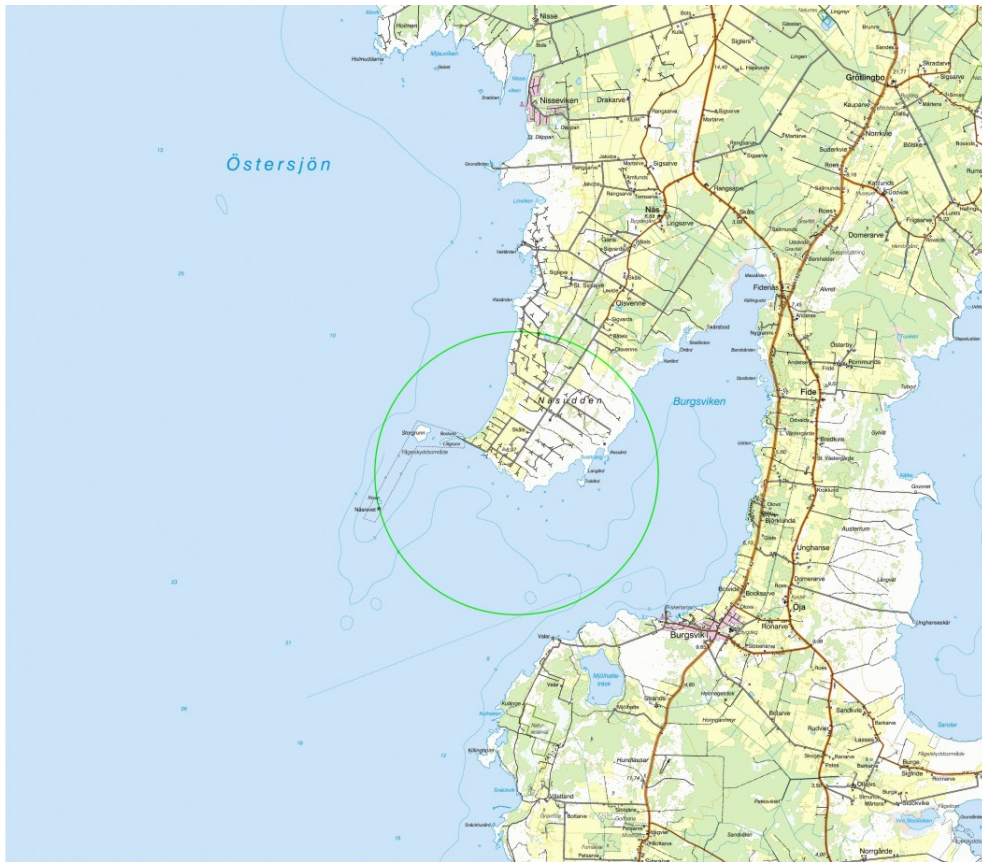
Figure 5.2: Näsudden, [12].

landscape roughness and distance between one change and another. The roughness rose is hence manually produced.

The other two ways are similar to each other. One is the "area objects" option. With this method a background roughness is set (i.e., the most frequent roughness class). All landscape types that differ from the background are encircled and set with a predetermined roughness class. The Wind-PRO software later produces a wind rose automatically from the background roughness and the area objects. One could also use "line objects" where the user sets the roughness to the right and to the left of a thought line. With this line the the user encircles the same variations in the landscape as in the area objects option. In this report area objects are used which in combination with the maps in WindPRO, the onsite observations and aerial photos, create a good representation of the actual site.
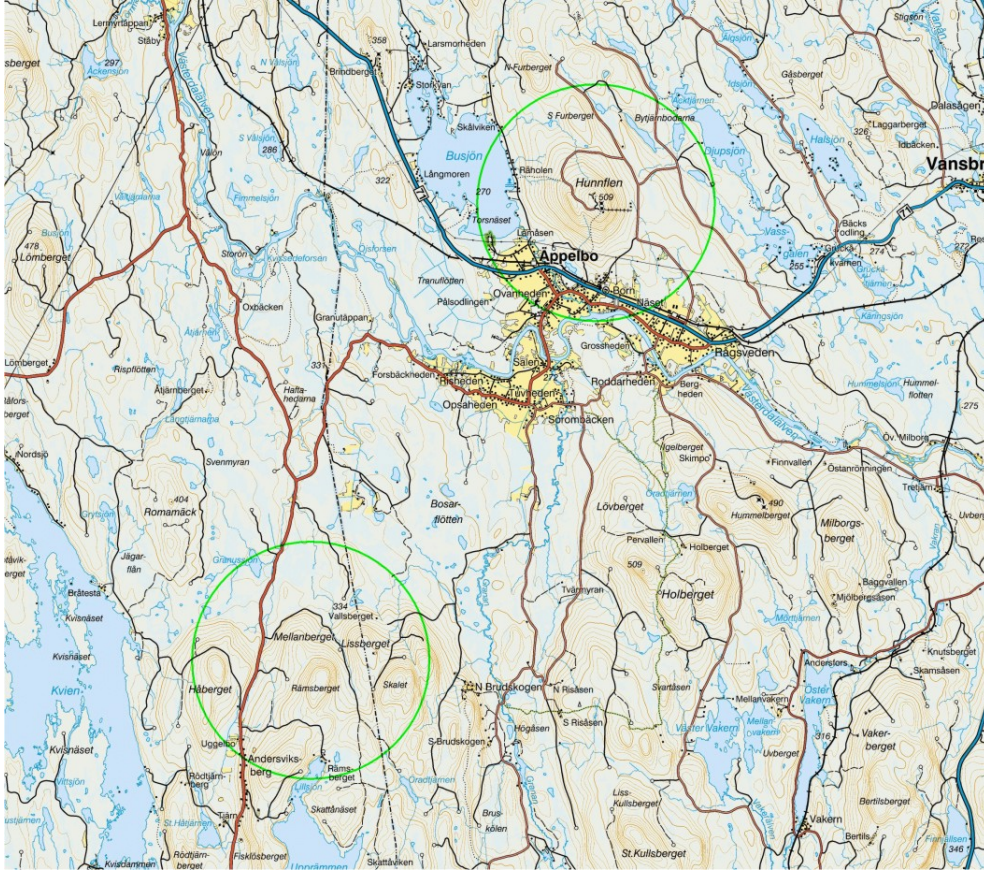
Figure 5.3: Hunnflen, [12].

5.1.4 Conversion of height contours and roughness class

Both height contours and roughness lines are converted into .map format. This is done only because both WAsP and WindSim require this format type in their simulations respectively.

5.2 Wind data

For the simulation of Siral at Näsudden, i.e., the low complexity simulation, it is difficult to find reliable wind data. Therefore, the wind data is extracted from WindPRO by using the given Weibull parameters. These are later transformed into a frequency table by a SciLab code written by the author, see appendix B. The wind data is taken from a mast that measured the wind from the year of 1980 to 1988 and was maintained by SMHI. The mast was

situated approximately 1,3 km from Siral. There is an uncertainty of the wind data due to extraction and transformation of the WindPRO data. However, the same wind data is used for both WAsP and WindSim simulation and the error margin in the wind data is equal for both simulations.

For the simulation of the wind turbines at Hunnflen, i.e., the high orograpgic complexity simulation, wind data is supplied by the local energy company. The data is given as wind speeds and directions at heights stretching from 20 up to 150 meters in 10 minutes intervals. The measuring mast is situated approximately 13 km away from Hunnflen at a mountain called Ramsberget. The measurement is performed during 2009 (and will therefore be compared to the energy production of 2009). The biggest error margin in this wind data is due to the distance between the wind turbine site and the measuring mast. However, the same wind data is used for both the WAsP and the WindSim simulation why the error margin is equal for both simulations.

5.3 Simulations

In this section the simulations will be presented.

5.3.1 Simulation in WAsP

In this section the WAsP simulations will be presented

Site Data   After converting the height contours and the roughness lines into .map format, there is an option to, within the WindPRO software, incorporate the WAsP model. WAsP is in other words executed inside WindPRO. Before the simulation, site data must be added. The site data will allow the user to incorporate the actual wind data.

Placement of turbines   The wind turbines have to be placed before the simulation can be started. WindPRO contains an extensive list of all of the most common wind turbine models. It is crucial to chose the correct wind turbine model since all turbines differ in terms of power curves, start and stop wind speeds, power control etc. Different models but with similar nominal output power would therefore show differences in energy production.

Energy production simulation   The energy production is finally simulated using the WAsP module in WindPRO. The results of the simulation are displayed in a series of documents in WindPRO.

5.3.2   Simulation in WindSim

To execute the simulation in WindSim mainly three files are needed; a terrain file in .gws format, a climatology file (which contains wind data), in either .wws or .tws format and a wind turbine power curve file in .pws format. Before starting with the simulation the .map file created in WindPRO has to be converted into .gws format. There are no possibilities, yet, to create the terrain file in WindSim directly. A third party software, such as WindPRO is needed in order to prepare the simulation.

Conversion of .map file

The conversion of the terrain file from .map to .gws format is however done in WindSim where the user defines the area of the simulation. This area should be as close to a square as possible and the side should be somewhere around 15,000 to 20,000 m. The terrain file is after conversion automatically added in the simulation project.

Modules

The simulation in WindSim consists of 6 modules. Each module, with some exceptions, is dependent on that the prior module is run. The section will present the 6 modules in WindSim.

Terrain   In this module a three dimensional terrain file will be created out of the .gws file. The user can in this module define the resolution of the simulation, both vertically and horizontally, by setting number of cells. Equation 5.1 shows how the maximum number of cells are determined.

$$n_x n_y n_z \leq n_{max} \tag{5.1}$$

In this case there are certain issues to be considered. Firstly, the time of the simulation is exponentially proportional to the number of cells. Secondly, the grid consists of many small cubes with a certain length in both x and y direction and a certain height in z direction. If the area in the conversion of the .map file into .gws format was chosen as a square then x and y should be approximately equal. The number of cells in z direction should be chosen so that the three dimensional cell is as close to a unit cube, i.e., with $x = y = z$. In fact, the ratio between the length and the height of the cube should never exceed 10 in order to complete the simulation without divergence, [9].

Wind Fields In this module the number of sectors is chosen. Normally, the number of sectors is equal the number of sectors in the climatology file which in most cases is 12. The flow will then be simulated for all sectors. This part of the simulation process is by far the most time consuming.

The height of boundary layer defines the height of the geostrophic wind which is set to 500 m by default. Furthermore, the speed above boundary layer height defines the geostrophic wind speed which is set to 10 m/s by default. The boundary condition at top should be set to fixed pressure at complex terrain and no-friction wall should be used at flat terrain

If a sector has not reached convergence after a selected number of iterations (see below) this sector can be re-simulated starting from the yet not converged solution from the previous run which in turn saves time. In the physical model the modified turbulence model is chosen as closure.

Furthermore, there are two different solvers; one coupled and one segregated. The coupled solver solves all the Navier-Stokes equations at the same time while the segregated one solves each equation at the time. The coupled therefore need less iterations in order to reach convergence but requires more time per iteration than the segregated one which in turn requires a lot more iterations. The result of the coupled and the segregated solver should however be the same if convergence is reach for both solvers for the same simulation, the coupled solver is however more sensitive when it comes to divergence, i.e., it can be more difficult to reach convergence with the coupled solver, [9]. The convergence monitoring is controlling a chosen parameter, e.g. speed scalar XYZ, at a chosen point preferably close to where the wind turbine is supposed to be placed.

Objects In this module climatologies and wind turbines are placed at desired places. In WindSim there are some predetermined power curves for a number of wind turbines. If the actual turbine does not exist in the list it can be created. The climatology normally consists of wind data, both mean speed and wind direction, from 12 sectors around the measuring mast. Each sector is then 30 degrees.

Results, Wind Resources and Energy After running the terrain, wind fields and objects modules, the results, wind resources and energy modules can be run. The Results module can be used to generate 3-dimensional pictures of the flow, the Wind resources module can be used to generate a wind resource map of the area and the Energy module can be used to calculate the annual energy production, AEP, of the chosen wind turbines.

Depending on what the user wants to extract from the program, the

proper module(s) are run. For instant, if the user wants to calculate the yearly energy production, the energy module should be run. If the user also wants to have a picture of the flow in 3D, the results module should be run. For the purpose of this report the Energy module is the most important since the yearly energy production is supposed to be compared to WAsP simulated and measured values.

5.4 Simulation results

The results are obtained and handled as annual energy production. To obtain the results in WAsP each simulation scenario is executed once. The simulation results in WindSim are dependent on the grid size. Therefore, the WindSim simulation consists of a grid sensitivity study. It is basically a multiple of simulations with varying grid size. The final result is then obtained when the AEP has converged, i.e., when the AEP is independent of the grid size. The simulations will start with a grid size of 5,000 cells which is increased until convergence is reached.

Chapter 6

Simulation sites

In this chapter the two different simulation sites will be presented.

6.1 Site A: Näsudden

Gotland has one of the highest densities of wind turbines in all of Europe and most of the turbines are located at Näsudden. The first wind turbine in the area was constructed in the beginning of the 80s. This turbine, named Albertina or Näsudden 1, was replaced by Matilda, or Näsudden 2, after 1991. Matilda was recently demolished due to a gear box breakdown but still holds the world record in energy production, 61,4 GWh, for a single wind turbine, [13].

6.1.1 Terrain type and roughness classification

The most typical landscape type at and in connection to Näsudden is the water. On land at the site of the turbines the dominating landscape type is open farm land. However, bushes and small trees are relatively common in the area. Figure 6.1 shows the roughness classification of Näsudden. The sea roughness is set to 0.5 and not 0 which is displayed on the map. This is done to cover for small islands and islets not included on the map.

6.1.2 Orography and height contours

When it comes to height variations, or orography, Näsudden is a low complexity area. The height difference between the sea line and the inner part of the peninsula is only at the size of about 10 meters vertically at a horizontal distance of 2 km. The height contours used for Näsudden have an

Figure 6.1: Roughness areas at Näsudden, [12].

equidistance of 1 meter, which means that the height difference between two adjacent lines is 1 meter. The height contours at Näsudden is shown in figure 6.2.

6.1.3 Wind conditions

Näsudden is listed as one of four areas on Gotland which are considered as national interests regarding wind power development. The predominant wind direction is south west as shown in figure 6.3.

6.1.4 Wind turbine: Siral

When chosing a wind turbine suitable for this simulation, the turbine has to be more or less unaffected by wind wakes from other turbines. It also has to
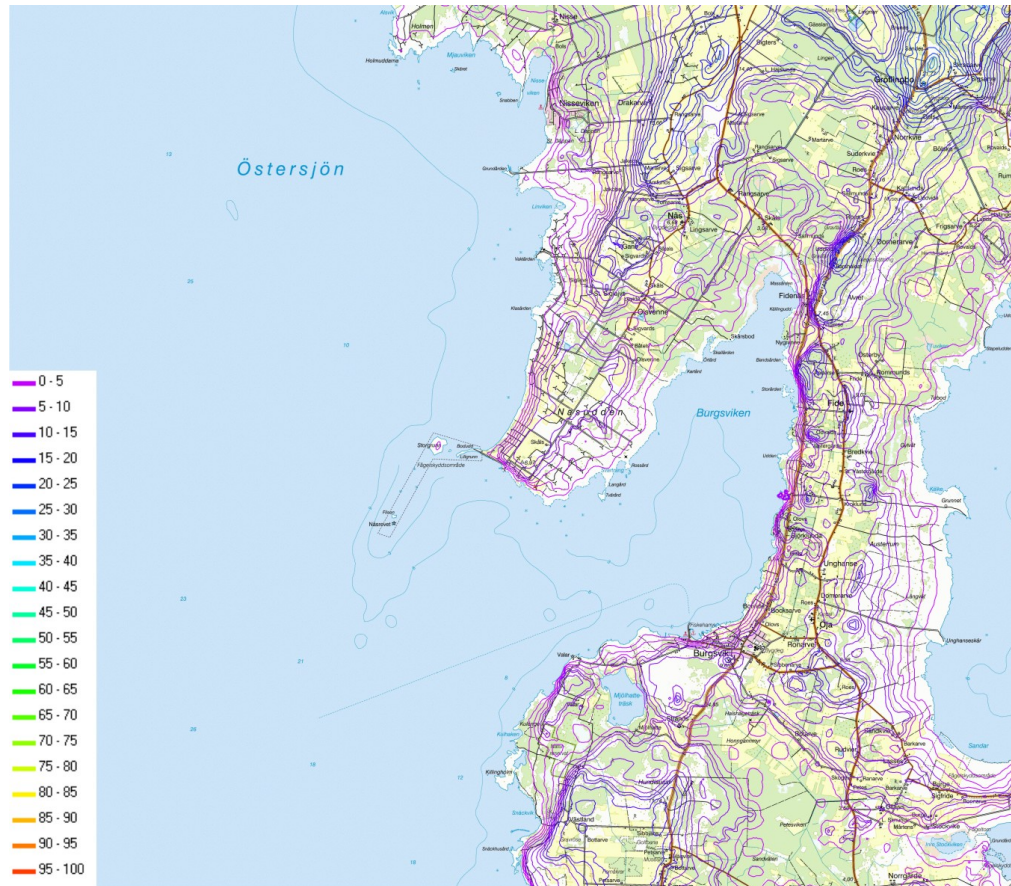
Figure 6.2: Näsudden with height contours [m.a.s.l.], [12].

have a couple of years of production data in order to be able to compare the simulated data to reliable production data. Siral is placed in the front line towards the predominant wind direction and is therefore most of the time unaffected, or very little affected, by wind wakes. The production data of Siral is also available from the year of 2002 to 2009 which is suffcient. Siral is a Vestas V42 model with a hub height of 41 m and a rotor diameter of 42 m. The turbine is equipped with an active pitch regulator and its nominal power is 600 kW, [18].

Measured annual energy production The measured average annual energy production of Siral is 1506 MWh per year. This average is calculated from the beginning of 2003 until end of 2009, which gives 7 years of data. The measured AEP varies from year to year and these variations are
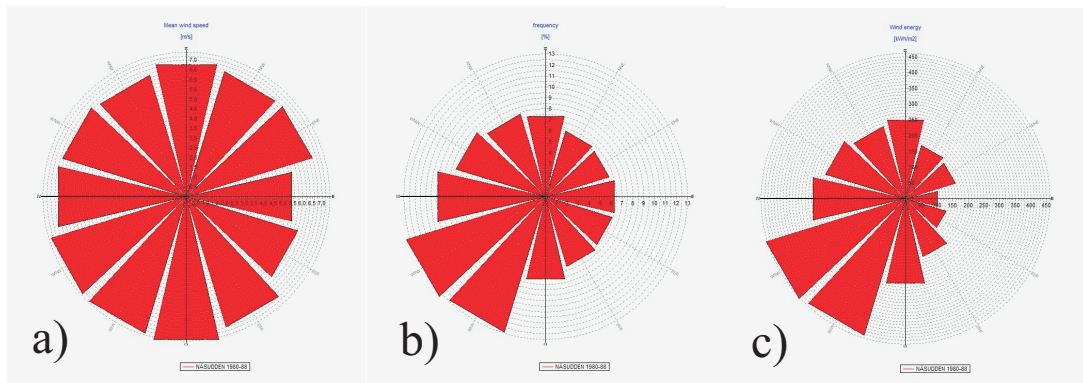
Figure 6.3: a) shows mean wind speed [m/s], b) frequency [%] and c) wind energy [kWh per square meter] at Näsudden for all 12 sectors, [Generated in WindPRO].

regarded as normal fluctuations in wind speed and frequency. However, in some cases it is obvious that the turbine has been out of order. If the average monthly production of 2006 is studied, one will find large deviations from the normal data. The hypothesis is that there have been operational difficulties during 2006. The production of 2006 is still included in the average production, and thus treated as a normal fluctuation, but one should keep in mind that increasing the production of 2006 to more normal values, would render a slightly higher average production per year. Figure 6.4 shows the yearly measured annual energy production and the average annual energy production, [18].
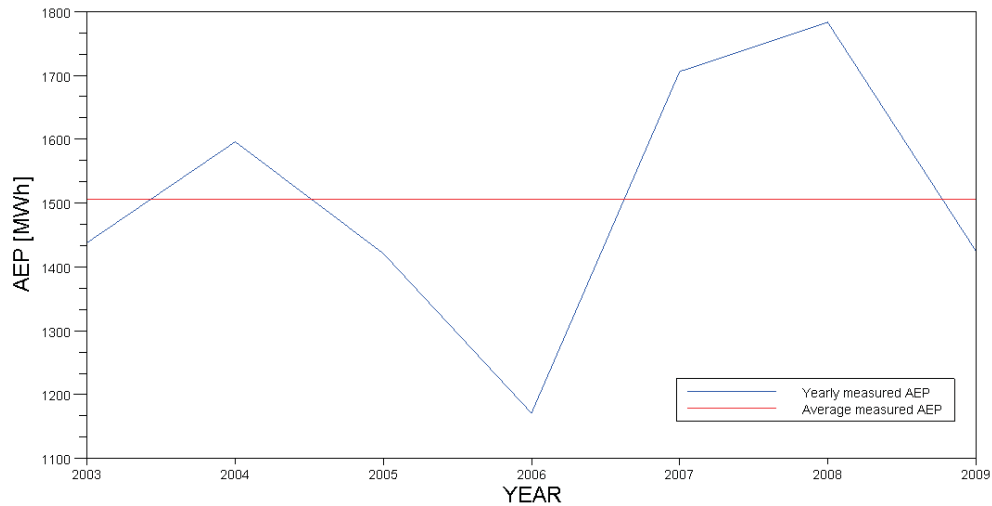
Figure 6.4: The measured annual energy production of Siral.

6.2 Site B: Hunnflen

The chosen wind turbine for the high complexity terrain simulations is located in Äppelbo, Dalarna , Sweden. The actual placement is a small mountain called Hunnflen which is used as a ski slope during winter. The landscape picture is therefore rather complex and suitable for this simulation. On the mountain there are smaller parties of forests which will have an impact on the simulations. There are three different wind turbines placed on the crest of the mountain.

6.2.1 Terrain type and roughness classification

The most typical terrain types at and in connection to Hunnflen are forest, swamp and lake. Forest are set as background roughness as it is the most common type. As the simulation is supposed to be run at a site with both high orographic complexity and with no forests the site is not ideal. However, to find a site matching both criteria is impossible. More important is the fact that both the WAsP and The WindSim simulations will be influenced by the forest in the same way. Figure 6.5 shows the roughness classification of Hunnflen.
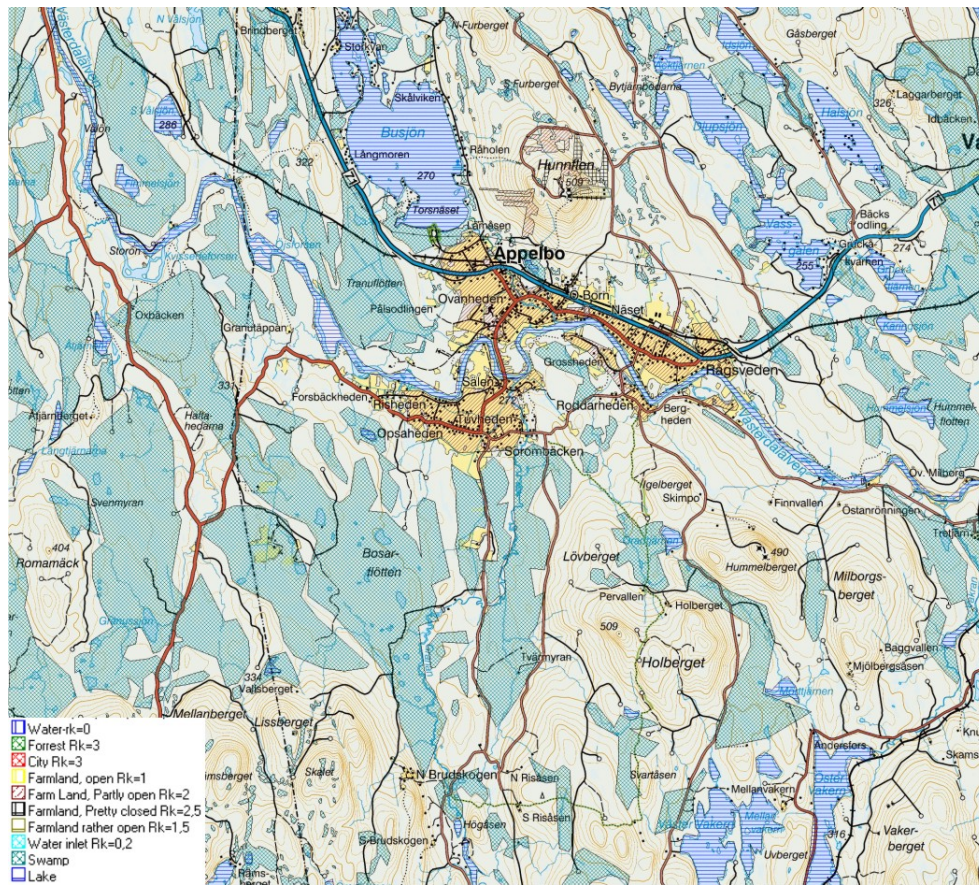
Figure 6.5: Roughness areas at Hunnflen, [12].

6.2.2 Orography and height contours

When it comes to height variations, or orography, Hunnflen is a complex area and in this aspect suitable for these evaluations. The height contours used for Hunnflen have an equidistance of 5 meter which is shown in figure 6.6.
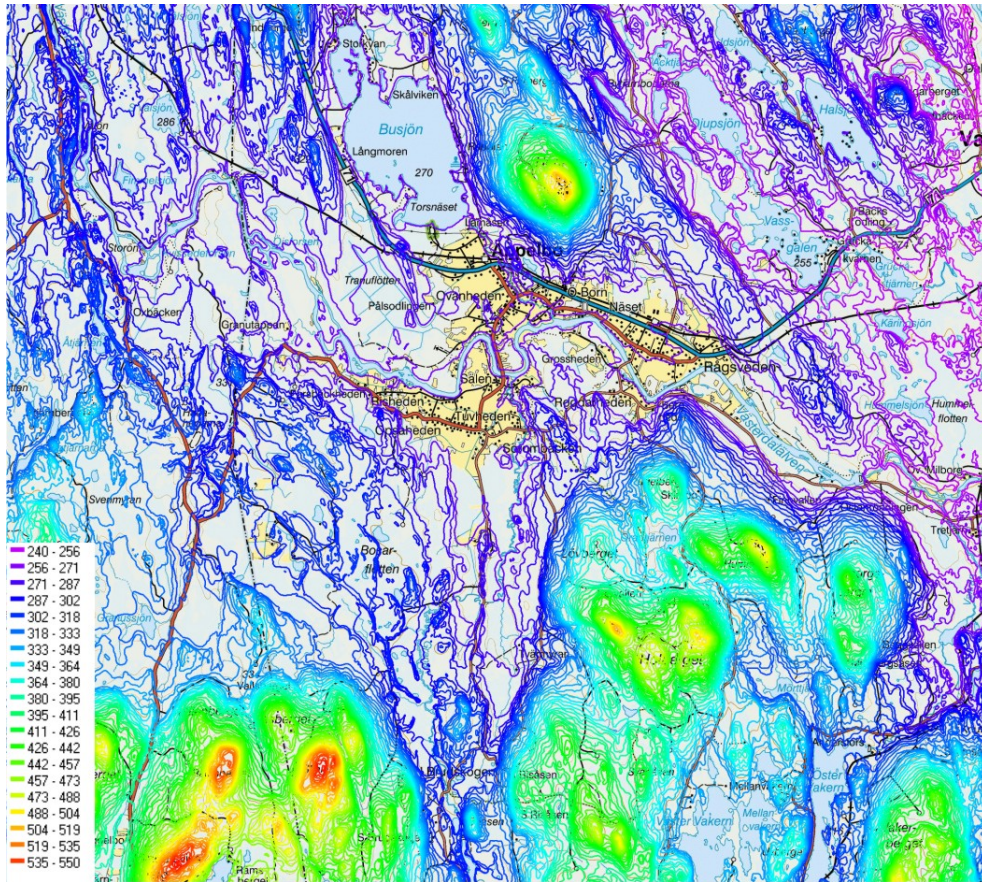
Figure 6.6: Hunnflen with height contours [m.a.s.l.], [12].

6.2.3 Wind conditions

6.2.4 Wind turbines

There are three turbines at the site which all have well documented production records. Therefore, all three turbines are chosen for this simulation, which allows using a wind wake option in the simulations.

There is one older turbine which was constructed in 2001 and was manufactured by NEG Micon. This turbine which is called Freja is a passive stall regulated turbine with a nominal power of 0,9 MW at a hub height of 49 m.

The other two was constructed in 2005 and was manufactured by Vestas. These turbines which are called Ferdinand and Vilhelm are similar when it comes to model and hub height. This model is pitch regulated and has nominal power of 0,85 MW. The hub height is 65 m, [18].
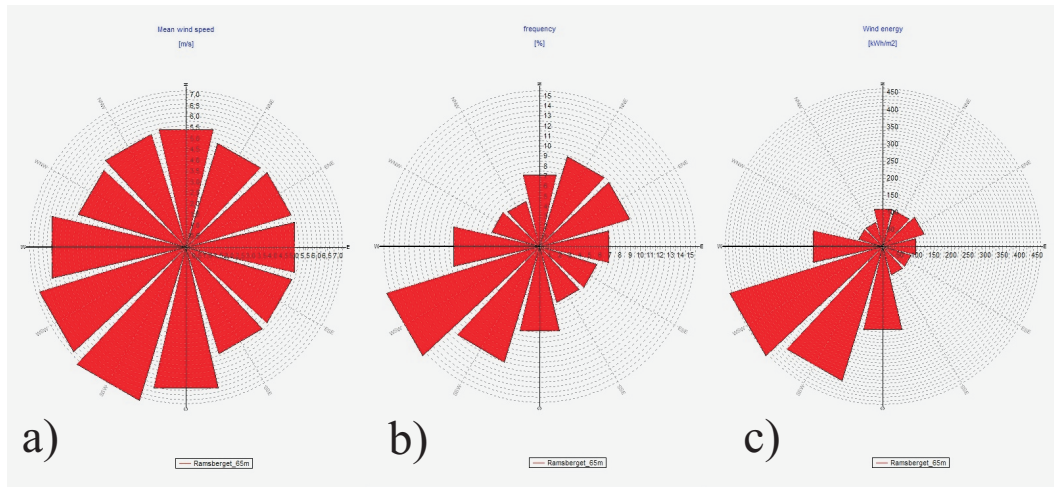
Figure 6.7: a) shows mean wind speed [m/s], b) frequency [%] and c) wind energy [kWh per square meter] at Hunnflen for all 12 sectors, [Generated in WindPRO].

Measured annual energy production In this section the measured production for the three different wind turbines will be presented. The average for Ferdinand and Vilhelm is calculated from the beginning of 2006 until the end of 2009. The average of Freja is calulated from the beginning of 2003 until the end of 2009. As for the measured production i Simulation A, there are certain periods when the wind turbines have been out of order. This is especially true for Freja during 2009 when its production is significally lower than the average production.

Ferdinand has the highest average measured annual energy production of the three wind turbines at Hunnflen. The average annual energy production is 2032,4 MWh per year. The annual energy production for 2009 is 1836,9 MWh. The annual energy production for 2009 is therefore about 90% of the average annual energy production ($\frac{1836,9}{2032,4} \approx 0,90$).

Ferdinand has the lowest measured average annual energy production of the three wind turbines at Hunnflen. The average annual energy production is 1728,6 MWh per year. The annual energy production for 2009 is 1607,6 MWh. The annual energy production for 2009 is therefore about 93% of the average annual energy production ($\frac{1607,6}{1728,6} \approx 0,93$).

The average annual energy production for Freja is 1911,9 MWh per year and the annual energy production for 2009 is 1474,6 MWh. The annual energy production for 2009 is therefore only about 77% of the average energy production ($\frac{1474,6}{1911,9} \approx 0,77$). This is significally lower than the other wind

turbines and by analyzing the production curve it can be stated that 2009 has been a very problematic year for Freja. If the annual energy production for 2009 is disregarded, the average annual energy production would instead become 1984,8 MWh per year. Since both Ferdinand and Vilhelm have a production of about 90% of the total average, a more accurate production of Freja would be $0,90 * 1984,8 \approx 1786,3$ MWh per year. This production is referred to as the corrected annual energy production. Both the measured and corrected annual energy production is used, [18].

Chapter 7

Results

7.1 Simulation A - Näsudden

Simulation A is performed in an area, Näsudden, with low orographic complexity. The simulation aims at determining differences between the two software due to the geographical situation. This section will therefore present the differences of annual energy production simulated by the software. Figure 7.1 shows a wind resource map over Näsudden created in WindSim. As one can see, the turbine, presented as the lower grey cone is placed in a spot with high mean wind speeds.
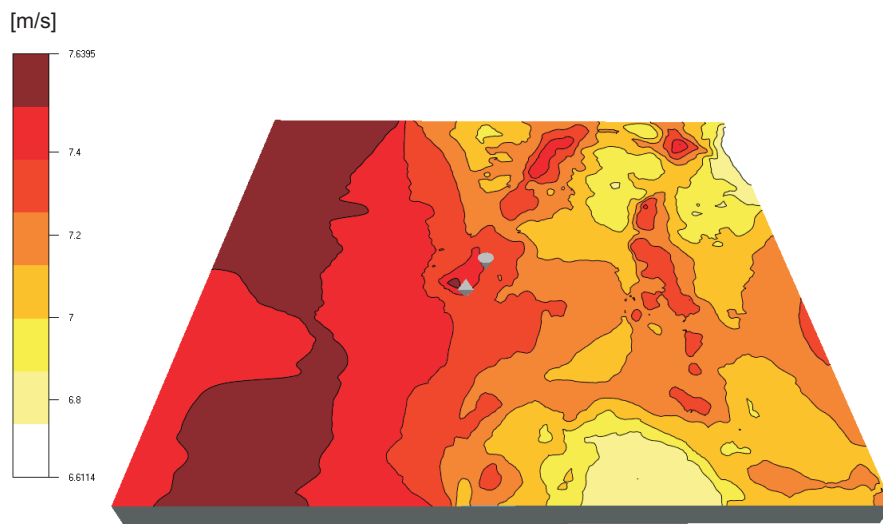

Figure 7.1: Wind resource map over Näsudden created in WindSim.

7.1.1 WAsP simulated annual energy production

The WAsP simulated AEP of Siral is 1513 MWh per year. This is treated as average production per year and is based on wind measurements which have taken place during several years.

7.1.2 WindSim simulated annual energy production

The WindSim simulated AEP of Siral is 1542 MWh per year. Since one can manually change the resolution of simulations in WindSim, a multiple of simulations have been run in order to determine the production and at which resolution this production is obtained, i.e., at which resolution the solution converges. Figure 7.2 shows how the simulated production varies with increased resolution. By regarding the graph it comes clear the simulated production is converged at a grid size of approximately 200,000 cells and at a production of approximately 1542 MWh per year. A grid size of 200,000 cells corresponds to a horizontal cell length of approximately 175 m in this case.
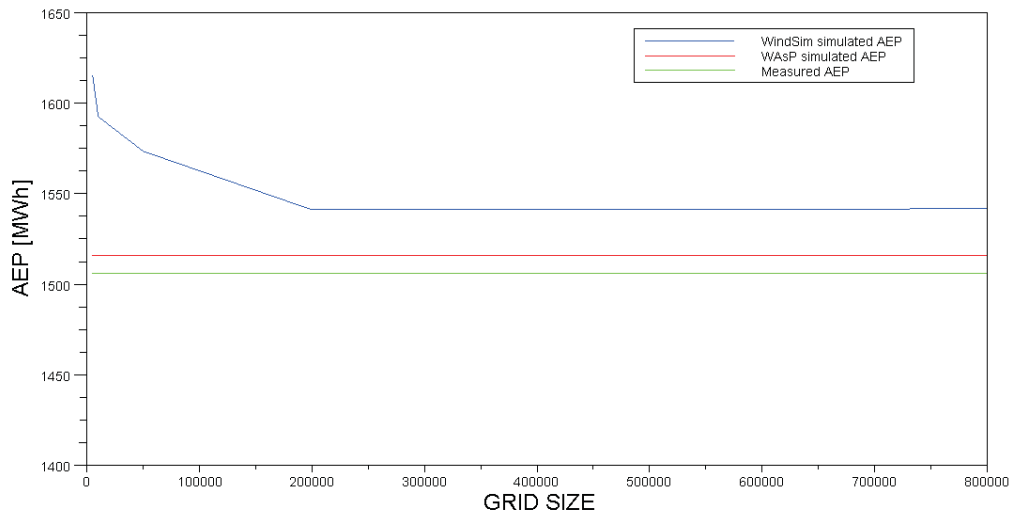

Figure 7.2: The WindSim simulated AEP of Siral.

7.1.3 Height coordinate variation

When changing the grid size, the resolution of the simulation changes. The terrain representation will be more accurate with higher grid sizes. It is therefore of interest to analyze how the height coordinate varies with grid size and it is especially interesting to determine when the height coordinate converges, i.e., when remains unchanged with increased grid size. At this point the accuracy of the terrain is as high as possible for the used terrain file. Figure 7.3 shows the height variation in relation to the grid size. The height coordinate converges at the same grid size as the energy production, i.e., at about 200,000 cells.
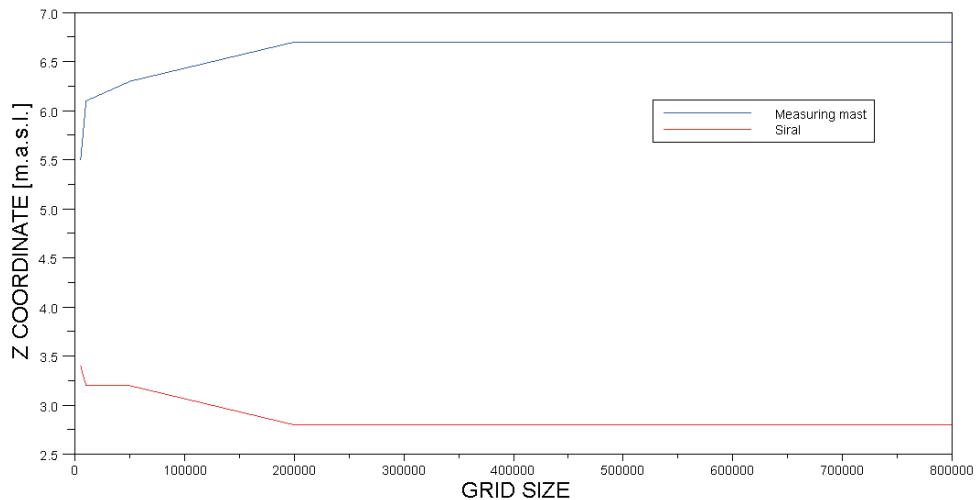
Figure 7.3: Height variation in WindSim simulation.

7.1.4 Comparing the software

When comparing the results, it can be stated that both software manage to estimate an energy production which is very close the measured one. The WAsP result is slightly better than the WindSim result but there are uncertainties in both the wind data and the measured production. Table 7.1 shows the differences between the software in simulated annual energy production.

Software	Measured AEP	Simulated AEP	Difference
WAsP	1506	1513	+0,5%
WindSim	1506	1542	+2,4%

Table 7.1: Measured production and simulation results for Siral.

7.2 Simulation B - Hunnflen

Simulation B is performed in an area, Hunnflen, with high orographic complexity. The simulation aims at determining differences between the two software due to the geographical situation. This section will therefore present the differences of the simulated annual energy production between the software. Figure 7.4 shows a wind resource map over Hunnflen created in WindSim. As one can see, the turbines, presented as the three grey cones in the north of the map are placed in spots with high mean wind speeds.
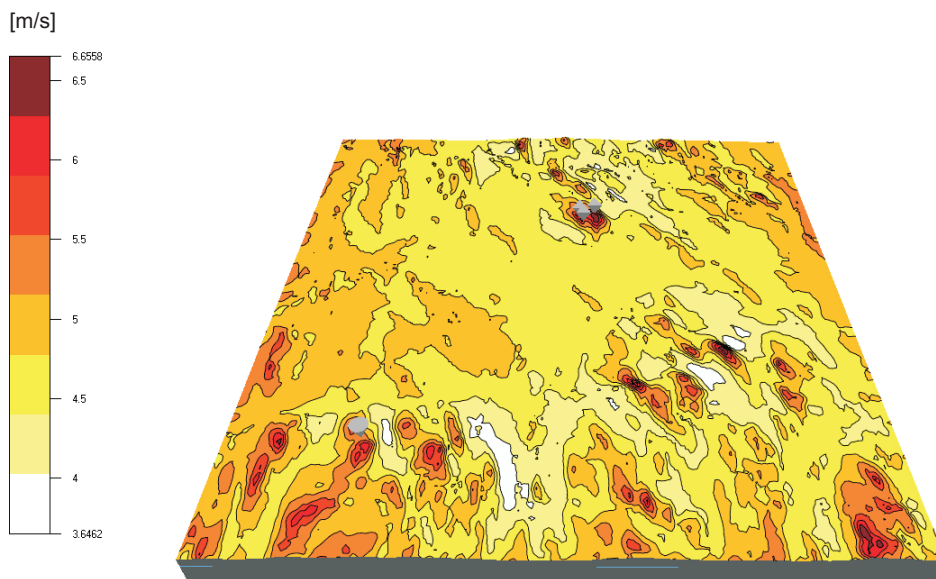

Figure 7.4: Wind resource map over Hunnflen created in WindSim.

7.2.1 WAsP simulated annual energy production

The WAsP simulation is performed with and without regarding wind wake interaction between the wind turbines. The results from the simulation is

presented in table 7.2 and show that the decrease in energy production due to wind wakes is very small.

Wind turbine	AEP without wakes	AEP with wakes	Wake decrease
Ferdinand	2538,6	2517,5	0,83%
Vilhelm	2349,0	2325,4	1,00%
Freja	2551,4	2515,7	1,40%

Table 7.2: WAsP simulated AEP.

7.2.2   WindSim simulated annual energy production

The WindSim simulation is as the WAsP simulation performed both with and without wind wake interaction. Since one can manually change the resolution of simulations in WindSim, a multiple of simulations have been run in order to determine the production and at which resolution this production is obtained, i.e., at which resolution the solution converges. Figure 7.5, 7.6 and 7.7 show how the simulated production varies with increased resolution for the different turbines. Table 7.3 presents the converged results for the different wind turbines. The annual energy production for Ferdinand and Vilhelm converges at a grid size of approximately 800,000 cells. A grid size of 800,000 cells corresponds in this case to a horizontal cell length of about 110 m.

   The energy production for Freja is not totally converged which is due to hardware limitations, the computer did not manage to execute a simulation with more cells than 1,000,000. However, by looking at the curve, one can see that it is about to level out and converge.

Wind turbine	AEP without wakes	AEP with wakes	Wake decrease
Ferdinand	1845,0	1837,0	0,43%
Vilhelm	1663,2	1656,9	0,38%
Freja	1815,3	1815,3	0,00%

Table 7.3: WindSim simulated AEP.

7.2.3   Height coordinate variation

When changing the grid size, the resolution of the simulation changes. The terrain representation will be more accurate with higher grid sizes. It is
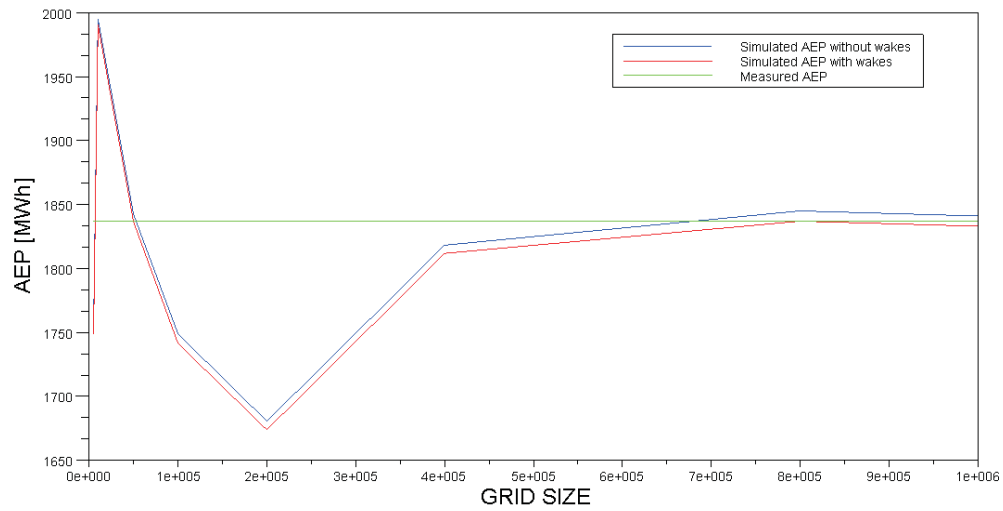
Figure 7.5: The WindSim simulated energy production per year of Ferdinand.
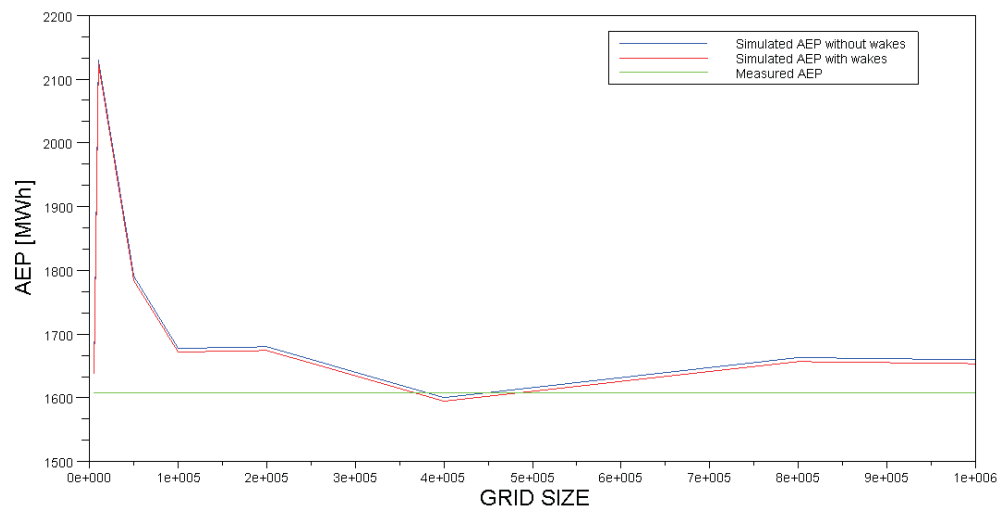
Figure 7.6: The WindSim simulated energy production per year of Vilhelm.

therefore of interest to analyze how the height coordinate varies with grid size and it is especially interesting to determine when the height coordinate

Figure 7.7: The WindSim simulated energy production per year of Freja.

converges, i.e., when remains unchanged with increased grid size. At this point the accuracy of the terrain is as high as possible for the used terrain file. Figure 7.8 shows the height variation in relation to the grid size. The height coordinate converges at a grid size of approximately 800,000 cells for the three turbines.

Figure 7.8: Height variation in WindSim simulation.

7.2.4 Comparing the software
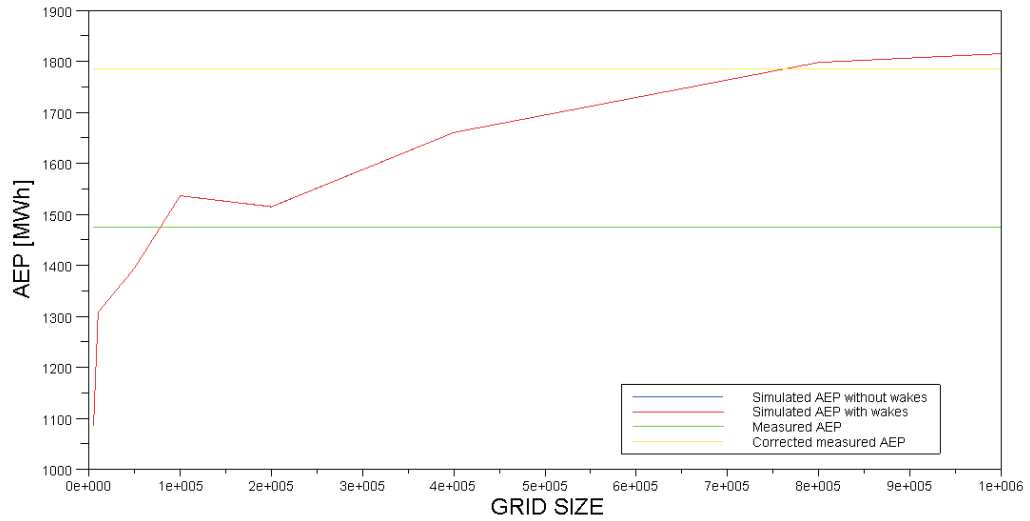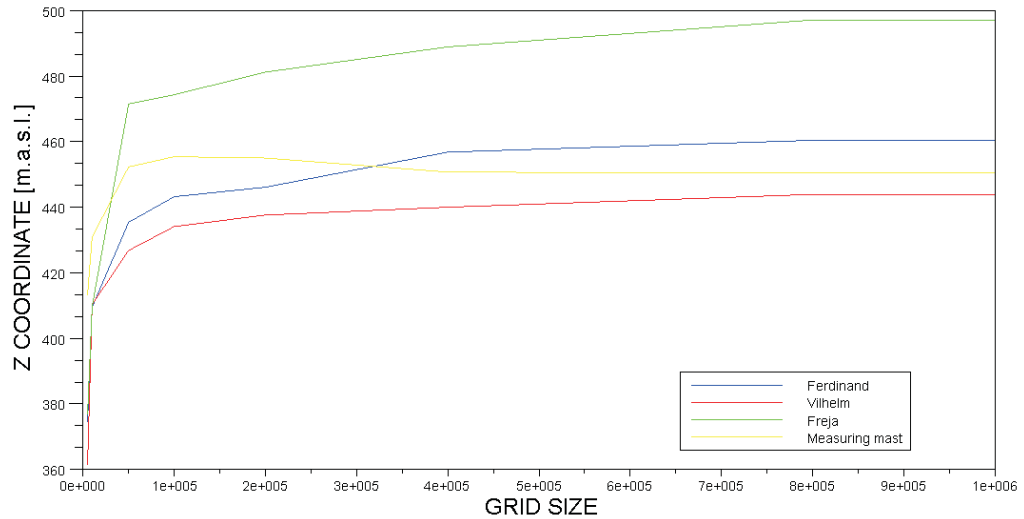
WAsP overestimates the energy production with about 700 MWh, or 40% for all the turbines. WindSim on the other hand manages to estimate an energy production which more or less corresponds to the measured one for all turbine if the corrected energy production of Freja is used. Again, one can state that wind wakes have a very low impact on the simulated energy production for both WAsP and WindSim. Table 7.4 and 7.5 show the WAsP simulated AEP without and with wind wake interaction. Table 7.6 and 7.7 show the WindSim simulated AEP without and with wind wake interaction. Figure 7.9 summarizes the simulated production for Hunnflen and Näsudden.

Wind turbine	Measured AEP	Simulated AEP	Difference
Ferdinand	1836,9	2538,6	+38,2%
Vilhelm	1607,6	2349,0	+46,1%
Freja	1474,6	2551,4	+73,0%
Freja corrected	1786,3	2551,4	+42,9%

Table 7.4: WAsP simulated AEP without wakes versus measured AEP.

Wind turbine	Measured AEP	Simulated AEP	Difference
Ferdinand	1836,9	2517,5	+37,1%
Vilhelm	1607,6	2325,4	+44,7%
Freja	1474,6	2515,7	+70,6%
Freja corrected	1786,3	2515,7	+40,8%

Table 7.5: WAsP simulated AEP with wakes versus measured AEP.

Wind turbine	Measured AEP	Simulated AEP	Difference
Ferdinand	1836,9	1845,0	+0,44%
Vilhelm	1607,6	1663,2	+3,46%
Freja	1474,6	1815,3	+23,1%
Freja corrected	1786,3	1815,3	+1,62%

Table 7.6: WindSim simulated AEP without wakes versus measured AEP.

Wind turbine	Measured AEP	Simulated AEP	Difference
Ferdinand	1836,9	1837,0	0,00%
Vilhelm	1607,6	1656,9	+3,07%
Freja	1474,6	1815,3	+23,1%
Freja corrected	1786,3	1815,3	+1,62%

Table 7.7: WindSim simulated AEP with wakes versus measured AEP.

7.3 Time consumption

In the low orographic complexity case it takes about 5 minutes to set up and perform the simulation in WAsP.

For WindSim, the time at 200,000 cells is therefore of interest since it is the lowest possible time needed to achieve a converged energy production. The convergence time noticed at sector 0-30 degrees (North) is about 23,5 min. This time is more or less the same for all 12 sectors why the total convergence time is $23,5 * 12 = 282 min = 4,7h$. A simulation performed without errors and re-runs at the current site will therefore take slightly less than 5 hours.

In the high orographic case WAsP consumes approximately 10 minutes to set up and perform the simulation.

For WindSim, the time at 800,000 cells is therefore of interest since it is the lowest possible time needed to achieve a converged energy production.
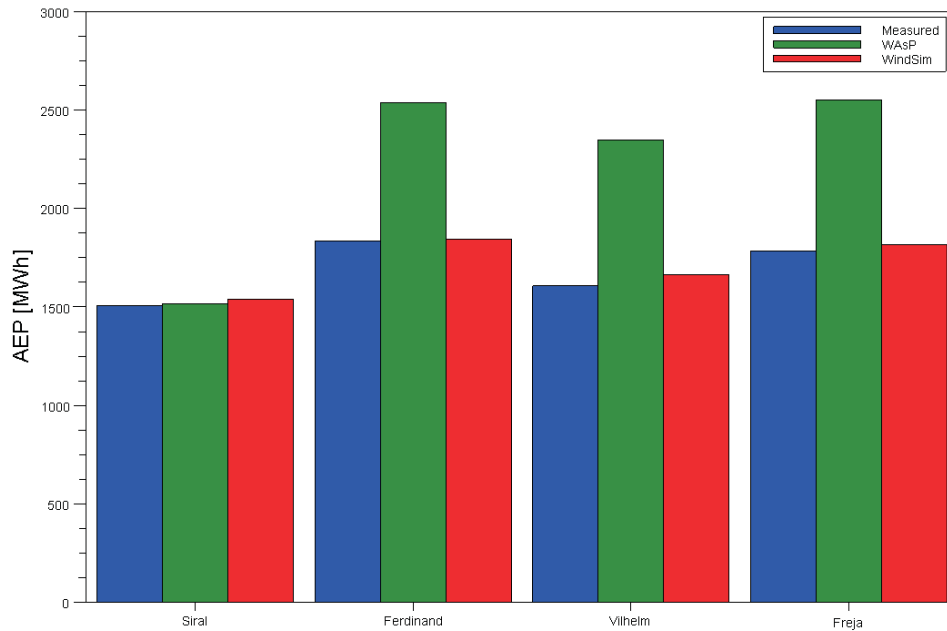
Figure 7.9: Measured and estimated energy production.

The convergence time noticed at sector 0-30 degrees (North) is about 24 min. This time is more or less the same for all 12 sectors why the total convergence time is $24 * 12 = 288min = 4,8h$. A simulation performed without errors and re-runs at the current site will therefore take slightly less than 5 hours.

In the simulation a desktop computer with a Intel Pentium Dual Core 2,5 GHz CPU and totally 4 GB of RAM has been used. The computer runs a 32-bit version of Windows Vista.

Chapter 8

Discussion

When it comes to orographic complexity one must keep in mind that the terrain model used is barely a simplification of the existing terrain. The same model, in this case represented by height contours, is used in both the linear and non-linear flow models. This report is therefore basically a study of how well each software can use this simplified model in its calculations for the chosen simulation parameter at the chosen location.

In the case for this project work, the measured energy production is known for all evaulation situations. In a normal case, wind resource maps, see section 2.3.3, are used to find a suitable site and is followed by wind measurements, see section 2.3.1, at the site. When wind data has been collected, the wind simulation software is used to estimate the annual energy production by transferring, see section 2.3.2, the measured wind data to the exact spot of the wind turbine. In this case there are no "answers" regarding the energy production, why the reliability of the software is vital.

8.1   Energy production

How well do the different software represent the measured annual energy production?

In the case of low orographic complexity it is evident that both simulation software estimate the measured annual energy production very well. In other words, the outcome of this study suggests that the choice of software does not matter if one look only at accuracy of estimation of energy production. However, WindSim requires a lot more simulation time. If this aspect is added to the energy production accuracy, this study gives an indication that WAsP should be used in the low orographic complexity case.

In the case of high orographic complexity the results differ significantly between the two software. WindSim estimates an energy production which is very close to the measured one but WAsP estimates an energy production which is about 40% too high.

The results is in line with what is stated in section 4.3 about differerences in the models. Both software manage to estimate the energy production accurately at Näsudden when the the terrain is flat, i.e., when the orographic complexity is low which depends on that the wind does not separate in this case since it exist only low angle slopes. In other words, the need for modeling turbulence, and thus for a turbulence model, is low in low orographic situations. In this case, the linear model, without the ability to model turbulence is as good as the non-linear model in wind energy estimation terms. Furthermore, the linear model much is in this case much more time efficient than the non-linear model which gives an indication that the linear model should be used in low orographic complexity cases such as the Näsudden case.

At the high orographic complexity case at Hunnflen the slope angles are in many cases larger than 17° and wind separation occures. In this situation the linear model overestimates the energy production since it cannot model the turbulence which is due to the wind separation. WindSim however, estimates the energy production with high accuracy even when wind separation occure due to its use of a turbulence model. In this case the results support the theory that a flow model that can model turbulence is necessary for an accurate energy estimation.

The three turbines at Hunnflen, are placed in a certain pattern and if one look at the measured production also this shows a certain difference. An interesting aspect is that WindSim also manages to reproduce this difference of production between the turbines.

8.2 Terrain

If one look at figure 7.3 and figure 7.8 it can be stated that the z coordinate for a given x and y coordinate varies greatly depending on the grid size. At a certain grid size the z coordinate stabilises and remains unchanged with increased grid size. According to the results of the simulation it can be stated that there is a correlation betweeen the stabilization of the z coordinate and the estimated energy production since they converge at the same grid size for all the performed simulations. It is however impossible to determine the interdependency between these variables with only the results from the performed simulations.

8.3 Convergence and time

In the low complexity simulation the AEP converges at a grid size of 200,000 cells and in the high complexity simulation the AEP converges at a grid size of 800,000 cells. Therefore, one can draw the conclusion that increased complexity leads to a need for an increased grid size to reach convergence. The time, however, which is needed to reach convergence is dependent on both the number of iterations as well as the grid size. Therefore, as stated in the results chapter, the time for the two simulations is approximately the same which is due to that the flow variables in the high orographic complexity case converged after less iterations than in the low orographic complexity case. The reason for this is unknown, a first idea was that the use of height contours with 1 meter of equidistance was the reason. By reducing the number of height contours so that the equidistance became 5 meter, as in the high orographic complexity case, the high number of iterations needed remained the same, so this was obviously not the case.

8.4 Uncertainties

Wind energy conversion is, like stated in the theoretical part of this report, a highly complex area in which a large number of parameters are involved. Energy estimation through various models is therefore also highly complex. In this report only one of these parameters is chosen to study; orographic complexity. By focusing on orographic complexity other parameters, such as roughness, are either neglected or not thouroghly analyzed. This poses uncertainties on the results. For instance, the roughness classification is probably the most subjective part of the simulation process and is therefore a source of uncertainty whether thouroghly analyzed or not. By focusing on the roughness classification this uncertainty can however be minimized which is not the case in this report. The same roughness classification has been used for both the software. The uncertainty due to this factor is therefore the same for both software.

The data, such as wind data and terrain data, used in the simulations does also pose uncertainties on the results. For instance, wind data is only valid for the measurement period and normally, the user wants to predict the energy production at a future site. This can only be done by using data from the past, why there are always inaccuracies in the resuts. The same wind data have been used for both software why the uncertainty due to this factor is the same for both software.

Like stated in the preamble of this chapter, the terrain file is only of a

model, a simplification, of the actual terrain. By using a model, there will be additional uncertainties in the results.

Other uncertainties lie in the author's previous experience with flow modelling, which was at a basic level in the beginning of the project. An effort has however been made to minimize these uncertainties by consulting experienced users and experts in the field of knowledge whenever needed in the project process.

8.5 General usage

One of the major disadvantages with WindSim is that there is no possibility to digitilize height contours and surface roughness. The software relies on a third party software such as WindPRO or WAsP to perform simulations. The economic cost for WindSim is therefore high. WAsP, on the other hand, does not need a third party software for its simulations.

8.6 Recommendations

For further studies in the field of this report, it is recommended to increase the number of simulation sites to cover for orographic complexities that lie between low and high. The validity of the results would be improved by doing so.

It would also be interesting to determine the exact relation between estimation of energy and stabilization of the terrain. The hypothesis is that the energy production is dependent of the stabilization of the terrain, i.e., the terrain is the dominant term. If this is the case, one could easily compare the z coordinate at a certain grid size with the actual measured z coordinate. If they correspond one can draw the conclusion that the resolution of the grid size is sufficient and that the energy production will be accurate. This would save time for the end user since sensivity studies become redundant.

Chapter 9

Conclusions

WAsP, which is based on a linear model, simulates the energy production with a high accuracy at low orographic complexity in a fast and efficient manner. When it comes to high orographic complexity WAsP does not manage to simulate the energy production with a satisfying accuracy. Therefore, WAsP can and should be used at low orographic complexity sites but not at the high complexity site since it cannot simulate turbulence which is of great importance at high orographic complexity sites.

WindSim, which is based on a non-linear model, simulates the energy production both at the low and high orographic complexity sites with high accuracy. WindSim is very time consuming in comparison to WAsP why it is especially usable at the high complexity site since it can model turbulence.

At the low orographic complexity case, the energy production in WindSim converges at around 200,000 cells. At the high orographic complexity case the energy production converges at around 800,000 cells. High orographic complexity therefore requires a larger grid than low orographic complexity in order to reach a converged solution.

Bibliography

[1] S. A. Ackerman and J. A. Know. *Meteorology: Understanding the Atmosphere*. Thomson Brooks/Cole, Pacific Grove, CA, 2003.

[2] D. C. Ahrens. *Meteorology today: an introduction to weather climate and the environment*. Cengage Learning, Minneapolis, 2007.

[3] H. Bergstrom. Vindkartering. http://www.energimyndigheten.se/. Accessed: 2010-04-01.

[4] J. Bogren. *Klimatologi, meteorologi*. Studentlitteratur, Lund, 1999.

[5] G. Britse. http://www.windpowerphotos.com. Accessed: 2009-12-01.

[6] EMD. EMD. http://emd.dk. Accessed: 2010-01-01.

[7] EMD. WindPRO. http://emd.dk/windpro/. Accessed: 2010-01-01.

[8] A. R. Gravdahl. Meso Scale Modeling with a Reynolds Averaged Navier-Stokes Solver. Documentation for WindSim users, 1998.

[9] A. R. Gravdahl. WindSim: Best Practices. Documentation for WindSim users, 2009.

[10] S. Ivanell. *Numerical Computations of Wind Turbine Wakes*. KTH Engineering Sciences, Stockholm, 2009, ISBN 978-91-7415-216-6.

[11] N. O. Jensen. *A Note on Wind Generator Interaction*. Risø National Laboratory, Roskilde, 1983.

[12] Metria. Digitala kartbiblioteket. https://butiken.metria.se/digibib/. Accessed: 2010-01-01.

[13] NyTeknik. Matilda faller for framtidens vindkraft. http://www.nyteknik.se/. Accessed: 2010-01-01.

[14] Risø. Facts about Risø. http://www.risoe.dk/. Accessed: 2009-12-01.

[15] Risø. WAsP. http://www.wasp.dk/. Accessed: 2009-12-01.

[16] R. B. Stull. *An Introduction to Boundary Layer Meteorology.* Kluwer Academic Publishers, Vancouver, 1988.

[17] I. Troen and E. L. Petersen. *European Wind Atlas.* Risø National Laboratory, Roskilde, 1989.

[18] Vattenfall. Driftsuppfoljning vindkraft. http://www.vindstat.nu. Accessed: 2010-04-01.

[19] Vindmolleindustrien. Power Control of Wind Turbines. http://guidedtour.windpower.org/. Accessed: 2010-01-01.

[20] T. Wallbank. Windsim validation study: CFD validation in complex terrain. Documentation for WindSim users, 2008.

[21] WindSim. History. http://www.windsim.com/. Accessed: 2009-12-01.

[22] WindSim. Product overview. http://www.windsim.com/. Accessed: 2009-12-01.

[23] WindSim. WindSim: The Basics. Documentation for WindSim users, 2009.

[24] T. Wizelius. *Vindkraft i teori och praktik.* Studentlitteratur, Lund, 2007.

Appendices
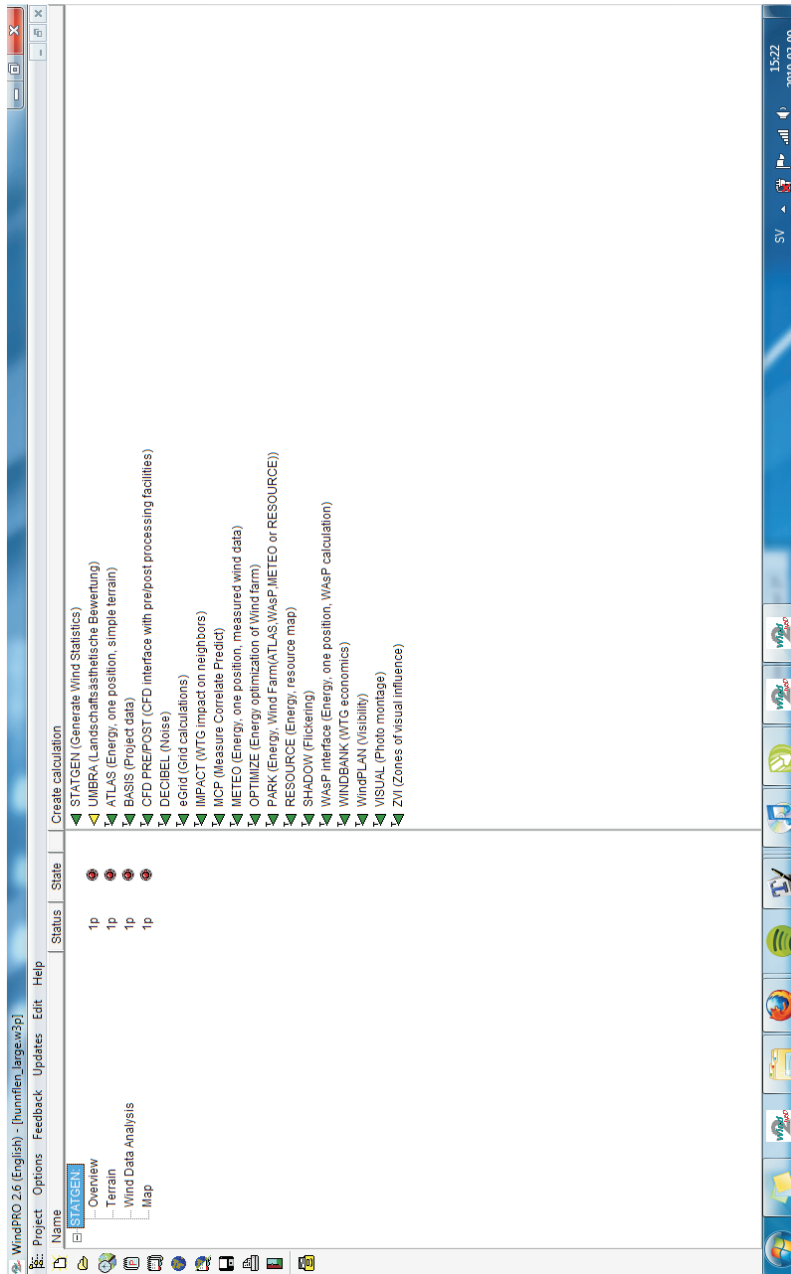
Appendix A

Software

A.1 WindPRO and WAsP

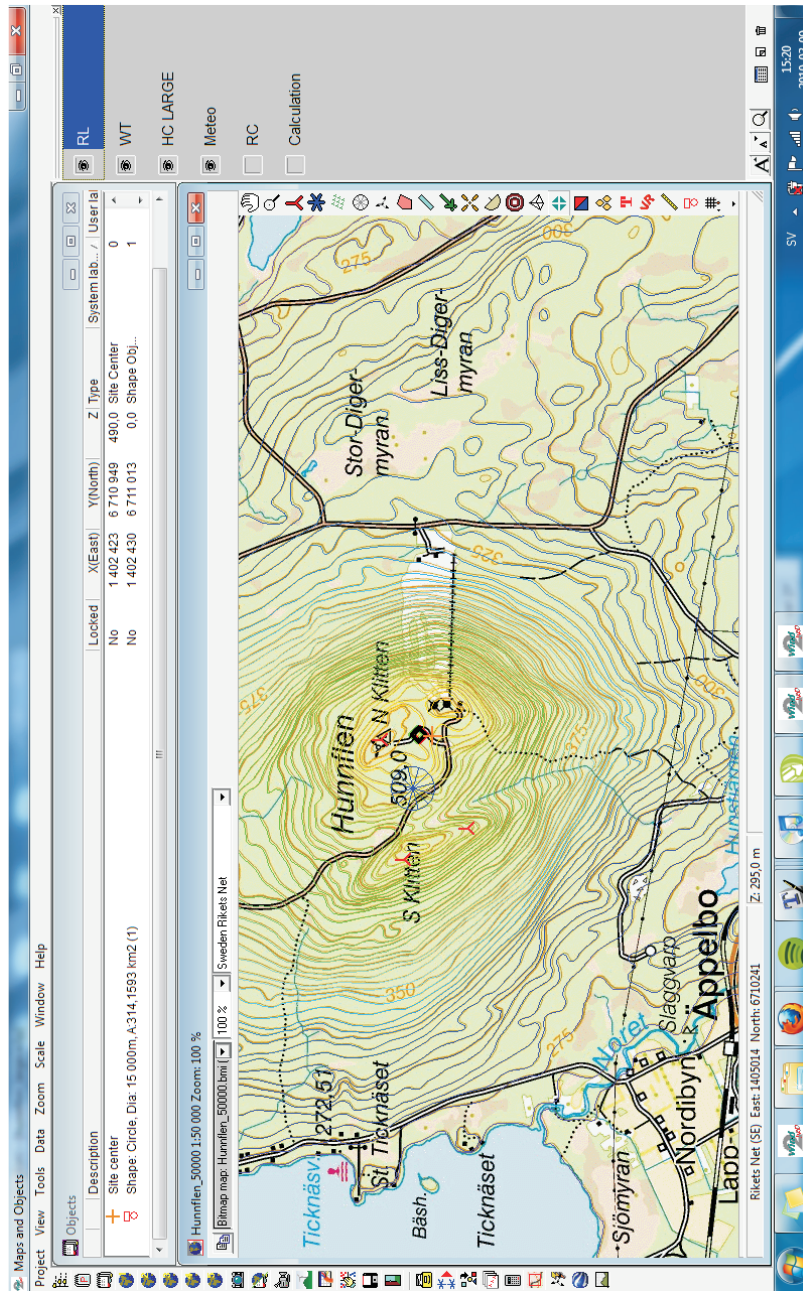**Figure A.1:** The WindPRO module interface.

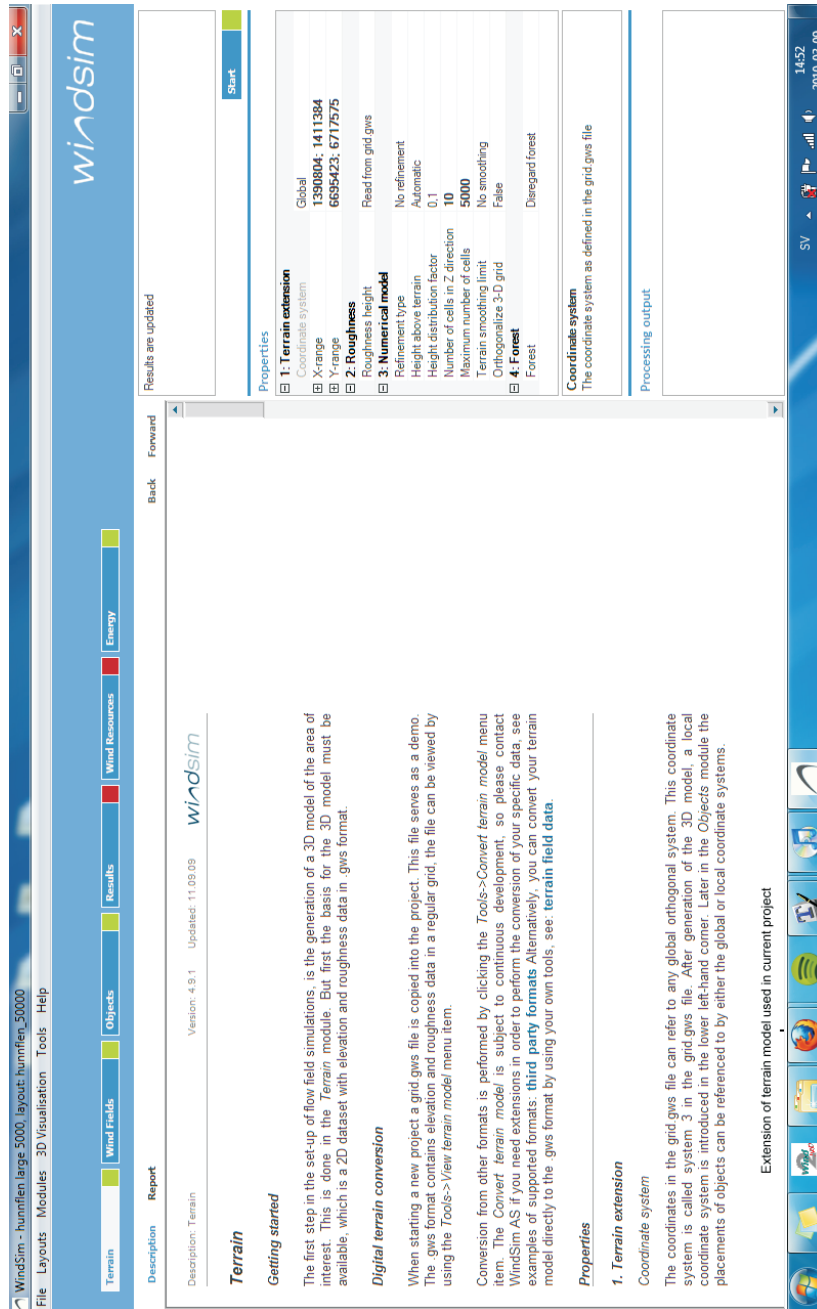**Figure A.2:** The WindPRO maps and objects interface.

A.2 WindSim

Figure A.3: The WindSim software interface.

A.2.1 Flow variables convergence

This section provides a picture on how the flow variables in WindSim converges. Figure A.4 shows the convergence picture for sector 0-30 degrees for the different grid size simulations that are conducted at Hunnflen, the high orographic complexity site for a certain spot. U1, V1 and W1 are wind speeds, KE is the turbulent kinetic energy and EP is the turbulent dissipation rate.
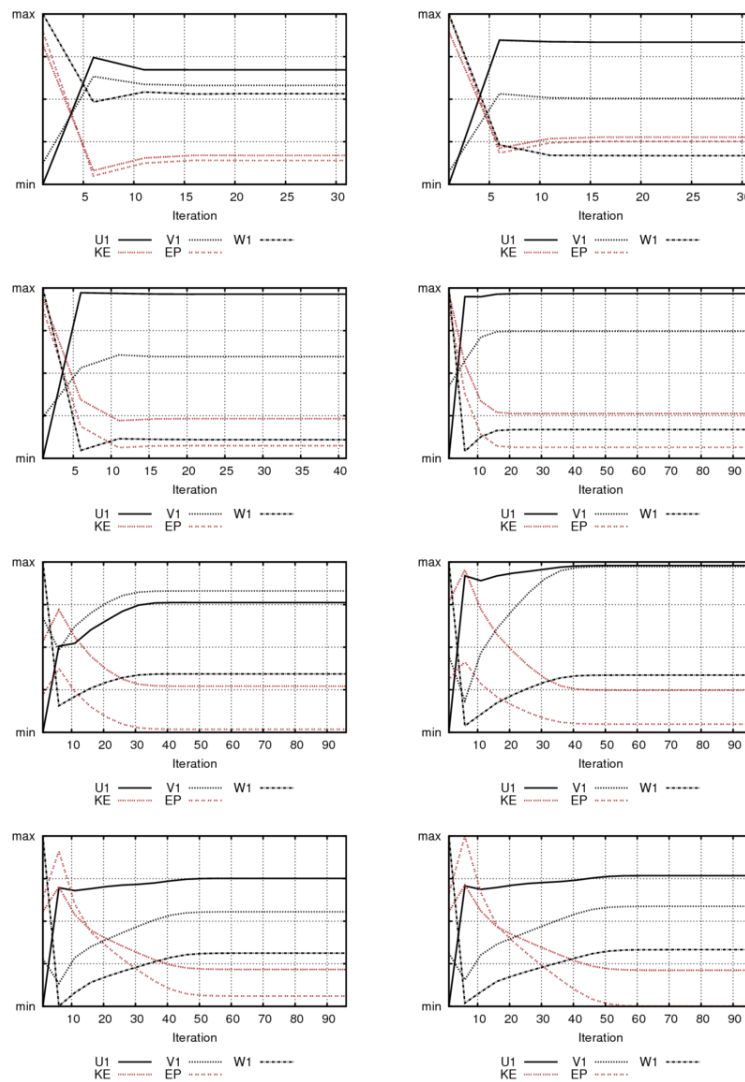

Figure A.4: The convergence for 5 of the flow variables for grid size 5,000, 10,000, 50,000, 100,000, 200,000, 400,000, 800,000 and 1,000,000 cells, respectively.

Appendix B

SciLab code

```
//INPUT BOXES FOR WEIBULL PARAMETERS AND FREQUENCY FOR EACH SECTOR
labels=["N" "NNE" "ENE" "E" "ESE" "SSE" "S" "SSW" "WSW" "W" "WNW" "NNW"];
[ok,k1,k2,k3,k4,k5,k6,k7,k8,k9,k10,k11,k12]=
getvalue("Define Weibull k shape parameter [-] for all sectors",labels,...
    list("vec",1,"vec",1,"vec",1,"vec",1,"vec",1,"vec",1,"vec",1,"vec",1,
"vec",1,"vec",1,"vec",1),["2";"2";"2";"2";"2";"2";"2";"2";"2";"2";"2";"2"]);

labels=["N" "NNE" "ENE" "E" "ESE" "SSE" "S" "SSW" "WSW" "W" "WNW" "NNW"];
[ok,A1,A2,A3,A4,A5,A6,A7,A8,A9,A10,A11,A12]=
getvalue("Define Weibull scale A parameter [m/s] for all sectors",labels,...
    list("vec",1,"vec",1,"vec",1,"vec",1,"vec",1,"vec",1,"vec",1,"vec",1,
"vec",1,"vec",1,"vec",1),["9";"9";"9";"9";"9";"9";"9";"9";"9";"9";"9";"9"]);

labels=["N" "NNE" "ENE" "E" "ESE" "SSE" "S" "SSW" "WSW" "W" "WNW" "NNW"];
[ok,per1,per2,per3,per4,per5,per6,per7,per8,per9,per10,per11,per12]=
getvalue("Define Weibull frequency [%] for all sectors",labels,...
    list("vec",1,"vec",1,"vec",1,"vec",1,"vec",1,"vec",1,"vec",1,"vec",1,
"vec",1,"vec",1,"vec",1),["0";"0";"0";"0";"0";"0";"0";"0";"0";"0";"0";"0"]);

//INPUT VALUES
k=[k1 k2 k3 k4 k5 k6 k7 k8 k9 k10 k11 k12];
A=[A1 A2 A3 A4 A5 A6 A7 A8 A9 A10 A11 A12];
per=[per1 per2 per3 per4 per5 per6 per7 per8 per9 per10 per11 per12]/100;

//MAKING ONE LARGE VECTOR OF THE 2 PARAMETER WEIBULL DENSITY FUNCTION
FOR EACH SECTOR
j=1;
for i=1:12
  x=0;
  while(x<30)
    y=k(i)/A(i)*((x/A(i))^(k(i)-1))*exp(-((x)/A(i))^k(i));
    z(j)=[y];
    x=x+0.01;
    j=j+1;
  end
end

//MAKING A 3000x12 MATRIX OF THE LARGE VECTOR DESCRIBED ABOVE
q=0;
for c=1:12
  z0(:,c)=[z(q+1:q+3000)];
  q=q+3000;
end

//MAKING A 30x12 MATRIX BY SUMMARIZING EVERY 100 POSITIONS IN
THE MATRIX DESCRIBED ABOVE
r=0;
for b=1:12
  a=3;
  z1(1,b)=[b];
  z1(2,b)=[per(b)];
  while(a<33)
    z1(a,b)=[sum(z0(r+1:r+100))/100*per(b)];
    a=a+1;
    r=r+100;
  end
end
```